A MULTI-BLADE MODEL FOR HELIOGYRO SOLAR SAIL STRUCTURAL DYNAMICS ANALYSIS

Jer-Nan Juang,* Jerry E. Warren,† Lucas G. Horta,† and William K. Wilkie†

An analytical model is derived to study the structural dynamic stability behavior for the free-flying heliogyro solar sail consisting of a finite set of symmetric or evenly distributed thin blades on a flat surface. Key properties of the flutter instability are described in terms of the relationship among the eigenvalues and eigenvectors associated with a flutter instability frequency. Various simulation cases for an idealized single blade, fixed rotational speed heliogyro model, and a generalized multi-bladed, freely spinning heliogyro model are presented to show how the flutter instability frequencies change as a function of the solar radiation pressure and the size of the dynamic model. Convergence of the flutter instability frequency versus the system order is demonstrated.

Keywords: solar sail, heliogyro, structural dynamics, stability.

INTRODUCTION

Solar sails are a propellantless in-space propulsion technology that produces thrust via momentum transfer of solar photons.[1–3] Recent NASA-sponsored research on the structural dynamics of the heliogyro has produced significant advances in understanding the coupled solar radiation pressure and structural dynamic ("solarelastic") stability behavior of heliogyro solar sails, including improved analytical and computational modeling capabilities, small-scale structural dynamics ground verification testing methods, and system identification procedures for on-orbit heliogyro blade dynamics investigations.[4–10]

In the early 1970s, the dynamic behavior of flexible spacecraft rotating in space was a problem of interest for aerospace researchers. For example, the Radio Astronomy Explorer (RAE/B) satellite consisted of a rigid hub attached with four cantilevered radial booms of equal length (approximately 230m each) possessing tip masses, and one pair of cantilevered damper booms. The spacecraft was free-spinning gravity-gradient stabilized. The stability analysis of the RAE consisted of: 1) the determination of the nontrivial equilibrium (or static deflection), 2) the calculation of a state-space model for describing the dynamic behavior with respect to the nontrivial equilibrium, and 3) the solution of the eigenvalue problem of the state-space matrix to determine the stability.[11–13] Variational equations of motion about the nontrivial equilibrium were derived by using the perturbed Lagragian in conjunction with the Lagrange's equations. Similarly, the proposed heliogyro solar

*National Institute of Aerospace, Hampton, VA 23666, USA; Honorary Professor, National Cheng Kung University, Tainan, Taiwan; Fellow AAS, AIAA, ASME
†Structural Dynamics Branch, NASA Langley Research Center, Hampton, VA 23681, USA

sail consists of six blades of equal length (220m each) attached to a hub. Both RAE and heliogyro spacecraft look similar in configuration but the heliogyro is free-spinning stabilized subject to a non-conservative external force, i.e., solar radiation pressure. Given the structural similarities between RAE and the heliogyro, the approach used to derive variational equations of motion for the RAE satellite can be directly applied for the stability analysis of the heliogyro spacecraft. Additional methods[14–16] that generate hybrid state equations of motion for flexible spacecraft in terms of quasi-coordinates may also be used.

Instead of using the perturbed Lagrangian,[12] Hamilton's principle is used in conjunction with generalized coordinates for deriving the variational equations of motion, discretizing the continuous variables, and solving the eigenvalue problem for stability analysis about a static deflection for the heliogyro. An analytical model was developed[4] earlier to describe the solarelastic behavior of an idealized, single-blade heliogyro model, and a symmetric two-blade heliogyro model. Fixed rotational speed and freely spinning hub boundary conditions were examined. This analytical model included dynamic coupling of rigid body motion of the central hub, radiation pressure forces, and the vibrational motion of the blades. For solarelastic stability analysis, a state-space matrix was obtained by discretizing the nonlinear dynamic model with continuous beam mode shapes and linearizing it with respect to the static deflection caused by the solar radiation pressure.

In this paper, the current continuous model is extended to include free-flying heliogyro configurations with a finite number of symmetric or evenly distributed thin blades. Fundamental equations are formulated yielding the mathematical relationship among the eigenvalues and eigenvectors associated with a flutter instability frequency. Unique features of the flutter instability eigenvectors will be shown such as their orthogonality with respect to the system state matrix. Various simulation cases will be presented using the extended model with; (1) an idealized single-blade heliogyro constant rotational rate case, (2) a symmetric, three-blade freely spinning heliogyro case, and (3) a symmetric, six-blade freely spinning heliogyro case. Convergence of flutter instability frequency will be shown against the number of beam modes for describing the vibrational motions of the blades. Comparisons between the instability characteristics of the free-spinning gravity-gradient stabilized RAE satellite and the free-spinning stabilized heliogyro configurations subject to solar radiation pressure will be discussed.

FREE SPINNING EQUATIONS OF MOTION FOR MULTIPLE BLADES

Figure 1 shows the basic configuration of the heliogyro solar sail with six blades attached to a rigid hub. Three coordinate frames are used to derive the heliogyro structural dynamic equations of motion. First is a blade coordinate frame to describe its corresponding blade deformation, second is the hub frame which is used to express the hub rotational motion, and third is the inertia frame for the translational motion of the origin of the hub frame.

An arbitrary position $\mathbf{r}_{k0}$ vector on the kth blade before deformation can be written by

$$\mathbf{r}_{k0} = R_x\mathbf{e}_{Ix} + R_y\mathbf{e}_{Iy} + R_{Iz}\mathbf{e}_{Iz} + H_{kx}\mathbf{e}_{kx} + x_k\mathbf{e}_{kx} + \eta_k\mathbf{e}_{ky} + \zeta_k\mathbf{e}_{kz} \tag{1}$$

and $\mathbf{r}_k$ after deformation is

$$\begin{aligned}\mathbf{r}_k \quad = \quad & R_x\mathbf{e}_{Ix} + R_y\mathbf{e}_{Iy} + R_{Iz}\mathbf{e}_{Iz} + H_{kx}\mathbf{e}_{kx} \\ & + \left[x_k + u_k - v_k' \left(\eta_k\cos\phi_k - \zeta_k\sin\phi_k\right) - w_k'\left(\eta_k\sin\phi_k + \zeta_k\cos\phi_k\right)\right]\mathbf{e}_{kx} \\ & + \left[v_k + \eta_k\cos\phi_k - \zeta_k\sin\phi_k\right]\mathbf{e}_{ky} + \left[w_k + \eta_k\sin\phi_k + \zeta_k\cos\phi_k\right]\mathbf{e}_{kz}\end{aligned} \tag{2}$$

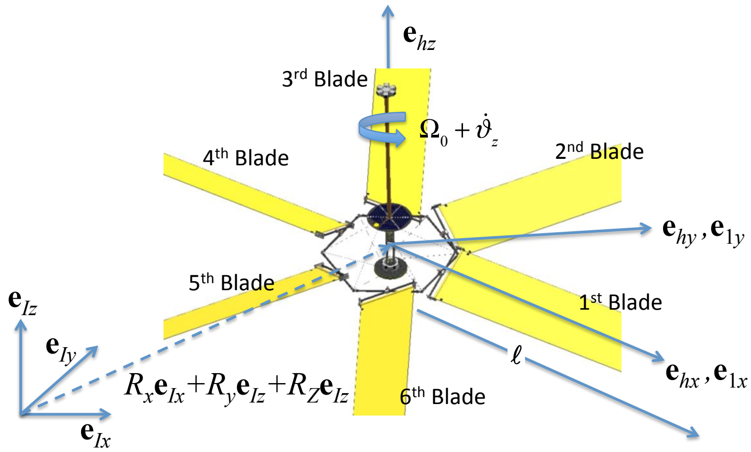

Figure 1. Idealized six-blade symmetric heliogyro configuration

for $k = 1, 2, \dots, n_b$ (number of blades). The variable H_{kx} is the distance from the center of the hub frame to the root of the kth blade frame. The variable x_k is the distance from the root of kth blade and u_k is the elongation displacement along the unit vector $\mathbf{e}_{kx}$, v_k is the in-plane displacement along the unit vector $\mathbf{e}_{ky}$ and w_k is the out-of-plane displacement along the unit vector $\mathbf{e}_{kz}$. Note that the position vector is derived using beam theory and all higher-order terms are ignored (see the order of variables in Appendix A and the section integrals in Appendix B).[3,17,18]

The position vectors shown in Eqs. (1) and (2) are used to derive the stress tensor for computing the blade strain energy $\mathcal{V}$. Taking the derivative of Eq. (2) with respect to time t gives the velocity for calculating the kinetic energy $\mathcal{T}$. Angular velocity $\boldsymbol{\omega}$ of the blade is expressed in terms of the hub frame as

$$\begin{aligned} \boldsymbol{\omega} \quad = \quad & \left[\dot{\vartheta}_x - \left(\dot{\vartheta}_z + \Omega_0\right)\sin\vartheta_y\right]\mathbf{e}_{hx} \\ & + \left[\dot{\vartheta}_y\cos\vartheta_x + \left(\dot{\vartheta}_z + \Omega_0\right)\cos\vartheta_y\sin\vartheta_x\right]\mathbf{e}_{hy} \\ & + \left[-\dot{\vartheta}_y\sin\vartheta_x + \left(\dot{\vartheta}_z + \Omega_0\right)\cos\vartheta_y\cos\vartheta_x\right]\mathbf{e}_{hz} \end{aligned} \tag{3}$$

Knowing the kinetic energy $\mathcal{T}$ and the strain energy $\mathcal{V}$ of the blade, Hamilton's principle yields variation quantities of $\mathcal{T} - \mathcal{V}$ in terms of $\delta R_x, \delta R_y, \delta R_z$ for translation, $\delta\vartheta_x, \delta\vartheta_y, \delta\vartheta_z$ for rotation of the hub frame, and $\delta u_k, \delta v_k, \delta w_k, \delta\phi_k$ for blade deflection with $k = 1, 2, \dots n_b$ (number of blades) that, in turn, produces the equations of motion. The inertial and blade coordiante frames involved in Eq. (2) can be transformed to the hub frame with a nominal spinning rate Ω_0 about the $\mathbf{e}_{hz}$ axis.

Using non-dimensional analysis as shown in Appendix C, consider that all non-dimensional deflection quantities are function separable, i.e

$$
\begin{aligned}
\bar{w}_k(\xi_k,\tau) &= \sum_{i=1}^{n} q_{w_k i}(\tau)\,\varphi_{w_k i}(\xi_k)\\
\bar{v}_k(\xi_k,\tau) &= \sum_{i=1}^{n} q_{v_k i}(\tau)\,\varphi_{v_k i}(\xi_k)\\
\bar{\phi}_k(\xi_k,\tau) &= \sum_{i=1}^{n} q_{\phi_k i}(\tau)\,\varphi_{\phi_k i}(\xi_k)\\
\bar{u}_k(\xi_k,t) &= \sum_{i=1}^{n} q_{u_k i}(\tau)\,\varphi_{u_k i}(\xi_k)
\end{aligned}
\tag{4}
$$

where $\tau = t/\Omega_0$ is a non-dimensional time and $1 \geq \xi_k = x_k/\ell \geq 0$ for all blades with equal length ℓ. The integer n is the number of beam mode shape functions, i.e., $\varphi_{w_k i}$, $\varphi_{v_k i}$, $\varphi_{\phi_k i}$, and $\varphi_{u_k i}$ for $i = 1, 2, \ldots, n$, which are used to approximate the out-of-plane, in-plane, twist, and elongation displacements of the kth blade.

Hamilton's principle produces the equations of motion including the linear and second-order nonlinear terms in the coefficients of the following matrix equation (see Appendix D),

$$
\bar{M}\ddot{q} + \bar{C}\dot{q} + \bar{K}q = \bar{f}_q \tag{5}
$$

where the quantity q is the non-dimensional generalized coordinate column vector

$$
q = \begin{bmatrix} \bar{R}_x & \bar{R}_y & \bar{R}_z & \bar{\vartheta}_x & \bar{\vartheta}_y & \bar{\vartheta}_z & q_{w_k i} & q_{v_k i} & q_{\phi_k i} \end{bmatrix}^T \tag{6}
$$

for $k = 1, 2, \ldots, n_b$, $i = 1, 2, \ldots n$, and $\bar{f}_q$ is the generalized force vector. The column vector q has a total of $6 + (3 \times n \times n_b)$ elements representing the degrees of freedom (i.e., the system order) of the whole system. Note that the elongation displacement u_k is not included in the coordinate vector, Eq. (6), because it is neglected in the process of deriving the matrix equation of motion, Eq. (5). Incidentally, the mass matrix $\bar{M}$, the gyroscopic matrix $\bar{C}$, and the nonlinear stiffness matrix $\bar{K}$ for a spinning blade are explicitly shown in Appendix D. The over bar on a quantity indicates that it is a non-dimensional quantity according to the nomenclature shown in Appendix C.

Generalized Force

The generalized force vector $\bar{f}_q$ consists of an internal centrifugal force and external forces due to the solar radiation force $\bar{p}_k$ applied at the kth blade. The internal centrifugal force is computed by neglecting the elongation displacement (see Appendix D). For the case where the vector of sun illumination is aligned with the spinning axis, the resulting generalized forces from virtual work are[17,18]

$$
\begin{aligned}
\delta\bar{f} &= \sum_{k=1}^{n_b} \int_0^1 (\bar{p}_k \cdot \delta\bar{r}_k)\, d\xi = \bar{f}_q \cdot \delta q\\
&= \begin{bmatrix} \bar{f}_{Rx} & \bar{f}_{Ry} & \bar{f}_{Rz} & \bar{f}_{\theta x} & \bar{f}_{\theta y} & \bar{f}_{\theta z} & \bar{f}_{w_k i} & \bar{f}_{v_k i} & \bar{f}_{\phi_k i} \end{bmatrix} \cdot\\
&\quad \begin{bmatrix} \delta\bar{R}_x & \delta\bar{R}_y & \delta\bar{R}_z & \delta\bar{\vartheta}_x & \delta\bar{\vartheta}_y & \delta\bar{\vartheta}_z & \delta q_{w_k i} & \delta q_{v_k i} & \delta q_{\phi_k i} \end{bmatrix}
\end{aligned}
\tag{7}
$$

where the non-dimensional generalized force vector $\bar{f}_q$ contains the generalized translational forces,

$$
\begin{aligned}
\bar{f}_{R_x} &= \sum_{k=1}^{n_b} \bar{p}_k \left[\bar{\vartheta}_y - \sum_{j=1}^{n} \left(q_{w_k j} \int_0^1 \varphi'_{w_k j} d\xi_k \mathrm{c}\theta_k + q_{\phi_k j} \int_0^1 \varphi_{\phi_k j} d\xi_k \mathrm{s}\theta_k \right) \right] \\
\bar{f}_{R_y} &= -\sum_{k=1}^{n_b} \bar{p}_k \left[\bar{\vartheta}_x + \sum_{j=1}^{n} \left(q_{\phi_k j} \int_0^1 \varphi_{\phi_k j} d\xi_k \mathrm{c}\theta_k - q_{w_k j} \int_0^1 \varphi'_{w_k j} d\xi_k \mathrm{s}\theta_k \right) \right] \\
\bar{f}_{R_z} &= \sum_{k=1}^{n_b} \bar{p}_k
\end{aligned}
\tag{8}
$$

the generalized rotational torques,

$$
\begin{aligned}
\bar{f}_{\vartheta_x} &= \sum_{k=1}^{n_b} \bar{p}_k \left(-\int_0^1 \xi_k d\xi_k \mathrm{s}\theta_k + \sum_{j=1}^{n} q_{vj} \int_0^1 \varphi_{v_k j} d\xi_k \mathrm{c}\theta_k \right) \\
\bar{f}_{\vartheta_y} &= -\sum_{k=1}^{n_b} \bar{p}_k \left(\int_0^1 \xi_k d\xi_k \mathrm{c}\theta_k + \sum_{j=1}^{n} q_{v_k j} \int_0^1 \varphi_{v_k j} d\xi_k \mathrm{s}\theta_k \right) \\
\bar{f}_{\vartheta_z} &= -\sum_{k=1}^{n_b} \bar{p}_k \left(\vartheta_x \int_0^1 \xi_k d\xi_k \mathrm{c}\theta_k - \vartheta_y \int_0^1 \xi_k d\xi_k \mathrm{s}\theta_k + \sum_{j=1}^{n} q_{\phi_k j} \int_0^1 \xi_k \varphi_{\phi_k j} d\xi_k \right)
\end{aligned}
\tag{9}
$$

and the generalized blade vibrational forces for the kth blade and ith mode,

$$
\begin{aligned}
\bar{f}_{q w_k i} &= \bar{p}_k \int_0^1 \varphi_{w_k i} d\xi_k \\
\bar{f}_{q v_k i} &= -\bar{p}_k \sum_{j=1}^{n} q_{\phi_k j} \int_0^1 \varphi_{v_k i} \varphi_{\phi_k j} d\xi_k;
\end{aligned}
\tag{10}
$$

where again $k = 1, 2, \ldots n_b$, $\mathrm{s}\theta_k = \sin\theta_k$ and $\mathrm{c}\theta_k = \cos\theta_k$. The quantity θ_k is the angle of the kth blade with respect to the first blade, assuming that all blades are located on a flat plane.

Note that coordinate-dependent terms in $\bar{f}_{Rx}, \bar{f}_{Ry}, \bar{f}_{\theta x}, \bar{f}_{\theta y}, \bar{f}_{\theta z}, \bar{f}_{q_{v_k i}}$ can be inserted into the stiffness matrix [see Appendix D, Eq. (D29)]. The term $\bar{f}_{q_{v_k i}}$ produces one-way coupling from twist to in-plane motion. The symmetry of the stiffness matrix is destroyed by these additional terms generated by the solar radiation pressure. The generalized constant force vector thus becomes

$$
\tilde{f}_q = \begin{bmatrix} 0 & 0 & \sum_{k=1}^{n_b} \bar{p}_k & -\frac{1}{2} \sum_{k=1}^{n_b} \bar{p}_k \mathrm{s}\theta_k & -\frac{1}{2} \sum_{k=1}^{n_b} \bar{p}_k \mathrm{c}\theta_k & 0 & \bar{p}_k \int_0^1 \varphi_{w_k i} d\xi_k & 0 & 0 \end{bmatrix}^T
\tag{11}
$$

where the last nonzero term inside the vector comes from the potential and kinetic energies associated with the variation of the out-of-plane displacement for the kth blade and ith mode. Moreover, the generalized constant forces for the rotational angles ϑ_x and ϑ_y, i.e., the fourth and fifth terms in Eq. (11) vanish when the multiple blades are evenly or symmetrically distributed. For example with $p_k = p_0 =$ constant for $k = 1, 2, \ldots, n_b$, $\cos(0) + \cos(120^o) + \cos(240^o) = 0$ for the three blades evenly distributed in a flat surface and located at 0^o, 120^o and 240^o, respectively. Thus, no static rotation takes place for the rotational angles ϑ_x and ϑ_y for the case of evenly or symmetrically distributed blades in a flat surface. Equations (1)-(11) are a complete set of dynamic equations for multiple blades.

Static Deflection

For cases where a constant solar radiation pressure is applied to the blades, for example, when the spin axis of the heliogyro is oriented towards the sun, a static deflection will occur. When the solar illumination is aligned with the spinning axis, the out-of-plane static deflection for the ith generalized coordinate of the kth blade can be solved linearly by

$$q_{w0_k i} = \left[\int_0^1 \bar{E}\bar{I}_w \varphi''_{w_k i} \varphi''_{w_k j} + \bar{T}_k \varphi'_{w_k i} \varphi'_{w_k j} - \bar{k}_{m1}^2 \varphi'_{w_k i} \varphi'_{w_k j} d\xi \right]^{-1} \left(\bar{p}_k \int_0^1 \varphi_{w_k i} d\xi_k \right) \tag{12}$$

for $i = 1, 2, \ldots, n$ and $k = 1, 2, \ldots, n_b$, assuming that all blades have identical material properties and configuration. Note that the system equations are nonlinear, i.e., there exists other static deflections that cannot be solved as easily as this one. This solution satisfies the nonlinear static equation for the constant spinning case of one blade. It is also valid for the case of multiple identical blades attached to the hub as shown in Fig. 1. Inserting the static solution, Eq. (5), into the system equations yields a linear matrix equation to solve for system eigenvalues to conduct stability and sensitivity analyses

MATHEMATICS OF SOLARELASTIC INSTABILITIES

The divergence instability is introduced first, and it follows by the flutter instability. Properties of flutter instability will then be discussed.

Divergence Instability

Without the presence of solar radiation pressure, Eq. (5), reduces to the linear matrix equation,

$$\bar{\mathscr{M}} \ddot{q} + \bar{\mathscr{C}} \dot{q} + \bar{\mathscr{K}} q = 0 \tag{13}$$

where $\bar{\mathscr{M}} = \bar{\mathscr{M}}^T > 0$ is a positive definite matrix, $\bar{\mathscr{C}} = -\bar{\mathscr{C}}^T$ is a skew symmetric matrix, and $\bar{\mathscr{K}} = \bar{\mathscr{K}}^T$ is a symmetric matrix. Its eigenvalue problem is

$$\left(\bar{\mathscr{M}} \lambda^2 + \bar{\mathscr{C}} \lambda + \bar{\mathscr{K}} \right) \psi = 0 \tag{14}$$

where λ is an eigenvalue and ψ is its corresponding eigenvector. Both eigenvalue and eigenvector may be real or complex numbers. Premultiplying Eq. (14) by the transpose of the eigenvector yields

$$\psi^T \left(\bar{\mathscr{M}} \lambda^2 + \bar{\mathscr{C}} \lambda + \bar{\mathscr{K}} \right) \psi = 0 \tag{15}$$

that produces the following equality

$$\lambda^2 = -\left(\psi^T \bar{\mathscr{M}} \psi \right)^{-1} \left(\psi^T \bar{\mathscr{K}} \psi \right) \tag{16}$$

Note that $\psi^T \bar{\mathscr{C}} \psi = \psi^T \bar{\mathscr{C}}^T \psi = -\psi^T \bar{\mathscr{C}} \psi = 0$. For the case where $\bar{\mathscr{K}} \geq 0$ (positive semidefinite), λ^2 is zero or a negative value, and thus λ is zero, or a pair of positive and negative pure imaginary number.

For the case where $\bar{\mathscr{K}} = \bar{\mathscr{K}}^T \not> 0$ or $\bar{\mathscr{K}} = \bar{\mathscr{K}}^T \not\geq 0$ (neither positive definite nor positive semidefinite), the quantity λ^2 can be a positive value such that λ is a positive or negative value implying that the system is in the state of *divergence instability*.

Flutter Instability

A non-zero solar radiation pressure $\bar{f}_q$ in Eq. (5) produces a static deflection, which results in the following matrix equation of motion for stability analysis with respect to the static deflection

$$\bar{\mathcal{M}}\ddot{q} + \bar{\mathcal{C}}\dot{q} + \bar{\mathcal{K}}q = \tilde{f}_q \tag{17}$$

where $\tilde{f}_q$ is shown in Eq. (11), and $\bar{\mathcal{M}}$, $\bar{\mathcal{C}}$, and $\bar{\mathcal{K}}$ are given in Eqs. (D26), (D27), and (D29) in Appendix D, respectively. The matrices $\bar{\mathcal{M}}$, and $\bar{\mathcal{K}}$ are not symmetric anymore. Inserting the out-of-plane static deflection $q_{w0_k i}$ for the ith generalized coordinate of the kth blade, computed in Eq. (12), and zero in-plane and twist static deflections, $q_{v0_k i} = q_{\phi 0_k i} = 0$, for $i = 1, 2, \ldots, n$ and $k = 1, 2, \ldots, k = n_b$ into the nonlinear terms in $\bar{\mathcal{M}}$ yields a constant matrix. These additional terms for the mass matrix $\bar{\mathcal{M}}$ are relatively small compared to other symmetric elements. Similar to the mass matrix, there are some additional terms added to the gyroscopic matrix due to the out-of-plane static deflection, but are small enough such that $\bar{\mathcal{C}} \approx -\bar{\mathcal{C}}^T$. As a result, Eq. (16) is still applicable, i.e., the eigenvalues and eigenvectors for Eq. (17) have the following property

$$\lambda^2 \approx -\left(\psi^T \bar{\mathcal{M}} \psi\right)^{-1} \left(\psi^T \bar{\mathcal{K}} \psi\right) \tag{18}$$

The stiffness matrix $\bar{\mathcal{K}}$ contains both nonlinear terms associated with the static deflection as well as linear terms directly contributed by the solar radiation pressure.

There exists a condition at a specific solar radiation pressure that a pair of complex eigenvalues are produced for λ^2,

$$\lambda^2 = \beta_R + i\beta_I; \quad \left(\lambda^2\right)^* = \beta_R - i\beta_I \tag{19}$$

The square roots of these complex numbers are

$$\lambda^2 = \beta_R + \beta_I i \Rightarrow \lambda = \pm \left(\sqrt{\frac{\beta_R + \sqrt{\beta_R^2 + \beta_I^2}}{2}} + i \frac{\beta_I}{|\beta_I|} \sqrt{\frac{-\beta_R + \sqrt{\beta_R^2 + \beta_I^2}}{2}} \right) \tag{20}$$

and

$$\left(\lambda^2\right)^* = \beta_R - \beta_I i \Rightarrow \lambda = \pm \left(\sqrt{\frac{\beta_R + \sqrt{\beta_R^2 + \beta_I^2}}{2}} - i \frac{\beta_I}{|\beta_I|} \sqrt{\frac{-\beta_R + \sqrt{\beta_R^2 + \beta_I^2}}{2}} \right) \tag{21}$$

There are two eigenvalues with a positive real part and nonzero imaginary part, implying that the system is unstable with oscillation, i.e., *flutter instability*. A flutter instability always comes with one pair (complex and its conjugate) of unstable modes and one pair of stable modes with the same frequency.

Properties of Flutter Instability

For the purpose of stability analysis, let the second-order matrix equation of motion, Eq. (5) , be transformed to the first-order matrix equation as

$$\dot{\bar{q}} = \bar{A}\bar{q} + \bar{f} \tag{22}$$

where

$$\bar{A} = \begin{bmatrix} \mathbf{0} & \mathbf{I} \\ -\bar{\mathcal{M}}^{-1}\bar{\mathcal{K}} & -\bar{\mathcal{M}}^{-1}\bar{\mathcal{C}} \end{bmatrix}; \bar{q} = \begin{bmatrix} q \\ \dot{q} \end{bmatrix}; \bar{f} = \begin{bmatrix} \mathbf{0} \\ \bar{\mathcal{M}}^{-1}\bar{f}_q \end{bmatrix} \tag{23}$$

and **0** and **I** are zero and identity matrices of appropriate dimension, respectively. Denote the four eigenvalues and eigenvectors corresponding to a flutter instability frequency as

$$\begin{bmatrix} \bar{\lambda} & \bar{\lambda}^* & -\bar{\lambda} & -\bar{\lambda}^* \end{bmatrix} \text{ and } \begin{bmatrix} \bar{\psi} & \bar{\psi}^* & \bar{\psi}_- & \bar{\psi}_-^* \end{bmatrix} \tag{24}$$

where the superscript $*$ means conjugate and all eigenvectors are normalized to the unit length, i.e., $\bar{\psi}'\bar{\psi} = \psi^{*\prime}\bar{\psi}^* = \bar{\psi}_-'\bar{\psi}_- = \bar{\psi}_-^{*\prime}\bar{\psi}_-^* = 1$. The flutter frequency has the following relationship among the eigenvalues and eigenvectors

$$\begin{cases} \bar{A}\bar{\psi} = \bar{\lambda}\bar{\psi} \\ \bar{A}\bar{\psi}_- = -\bar{\lambda}\bar{\psi}_- \\ \bar{A}\bar{\psi}^* = \bar{\lambda}^*\bar{\psi}^* \\ \bar{A}\bar{\psi}_-^* = -\bar{\lambda}^*\bar{\psi}_-^* \end{cases} \Rightarrow \begin{cases} \bar{\psi}'\left(\bar{A} + \bar{A}^T\right)\bar{\psi} = 2\mathrm{Re}\left(\bar{\lambda}\right) \\ \bar{\psi}_-'\left(\bar{A} + \bar{A}^T\right)\bar{\psi}_- = -2\mathrm{Re}\left(\bar{\lambda}\right) \\ \psi^{*\prime}\left(\bar{A} + \bar{A}^T\right)\bar{\psi}^* = 2\mathrm{Re}\left(\bar{\lambda}^*\right) \\ \bar{\psi}_-^{*\prime}\left(\bar{A} + \bar{A}^T\right)\bar{\psi}_-^* = -2\mathrm{Re}\left(\bar{\lambda}^*\right) \end{cases} \tag{25}$$

where the superscript $'$ means conjugate and transpose. The four equations are also true for any other system eigenvalue. For an eigenvalue with no real part, its eigenvector is rotated 90^o by the symmetric matrix $A + A^T$ such that the resultant vector is orthogonal to its own eigenvector. Before flutter or divergence occurs for a system without materials damping, its eigenvectors are orthogonal to the vectors transformed by the symmetric matrix, $A + A^T$.

Note that the matrix $A - A^T$ is a skew-symmetric matrix and thus

$$\begin{cases} \bar{\psi}^{*\prime}\left(A - A^T\right)\bar{\psi} = \bar{\psi}^T\left(A - A^T\right)\bar{\psi} = 0 \\ \bar{\psi}_-^{*\prime}\left(A - A^T\right)\bar{\psi}_- = \bar{\psi}_-^T\left(A - A^T\right)\bar{\psi}_- = 0 \end{cases} \tag{26}$$

The properties are also true for any real state matrix having a pair of complex eigenvalues with or without real parts. On the other hand, flutter eigenvalues always have both real and imaginary parts.

Key properties for eigenvectors with eigenvalues $\bar{\lambda}$ and $-\bar{\lambda}$, and $\bar{\lambda}^*$ and $-\lambda^*$, i.e., relationship of eigenvectors associated with stable and unstable eigenvalues

$$\begin{cases} \bar{\psi}_-'\left(\bar{A} - \bar{A}^T\right)\bar{\psi} = \left(\bar{\lambda} + \bar{\lambda}^*\right)\bar{\psi}_-'\bar{\psi} = 2\mathrm{Re}\left(\bar{\lambda}\right)\bar{\psi}_-'\bar{\psi} \\ \bar{\psi}_-^{*\prime}\left(\bar{A} - \bar{A}^T\right)\bar{\psi}^* = \left(\bar{\lambda}^* + \bar{\lambda}\right)\bar{\psi}_-^{*\prime}\bar{\psi}^* = 2\mathrm{Re}\left(\bar{\lambda}\right)\bar{\psi}_-^{*\prime}\bar{\psi}^* \end{cases} \tag{27}$$

Key properties for the eigenvectors with eigenvalues $\bar{\lambda}$ and $-\bar{\lambda}^*$, and $\bar{\lambda}^*$ and $-\lambda$, i.e., relationship of eigenvectors associated with stable and unstable conjugate eigenvalues

$$\begin{aligned} &\begin{cases} \bar{\psi}_-^{*\prime}\bar{A}\bar{\psi} = \bar{\lambda}\bar{\psi}_-^{*\prime}\bar{\psi} \\ \bar{\psi}'\bar{A}\bar{\psi}_-^* = -\bar{\lambda}^*\bar{\psi}'\bar{\psi}_-^* \end{cases} \Rightarrow \bar{\psi}_-^{*\prime}\left(\bar{A} + \bar{A}^T\right)\bar{\psi} = 0 \\ &\begin{cases} \bar{\psi}_-'\bar{A}\bar{\psi}^* = \bar{\lambda}^*\bar{\psi}_-'\bar{\psi}^* \\ \bar{\psi}^{*\prime}\bar{A}\bar{\psi}_- = -\bar{\lambda}\bar{\psi}^{*\prime}\bar{\psi}_- \end{cases} \Rightarrow \bar{\psi}_-'\left(\bar{A} + \bar{A}^T\right)\bar{\psi}^* = 0 \end{aligned} \tag{28}$$

The eigenvector $\bar{\psi}_-^*$ for the eigenvalue of $-\bar{\lambda}^*$ is orthogonal to $\bar{\psi}$ for the eigenvalue $\bar{\lambda}$ with respect to the symmetric matrix $A + A^T$. These special features provide a way to develop an algorithm to trace coupled modes for flutter-instability sensitivity analysis.

SIMULATION RESULTS

Nominal parameters for the heliogyro configuration (see Fig. 1) are given in Table 1. Using the

Table 1. Nominal Blade Parameters and Ranges

Parameters	Nominal	Upper Bound	Lower Bound
Length (m)	220	220	220
Thickness x 10^{-6} (m)	2.74	2.8085	2.6715
Width (m)	0.75	0.75	0.75
Density (kg/m^3)	1490	1527.25	1452.75
Modulus x 10^9 (N/m^2)	9.67	9.42825	9.91175
Mass Inertias Ixx, Iyy, Izz (kg m^2)	0.62	0.62	0.62
Hub Mass (Kg)	7.6	8.36	6.84
Solar Pressure x 10 $^{-6}$ (N/m^2)	10	15	5

nominal parameters, three cases are shown including one-blade constant spinning, three-blade free spinning, and six-blade free spinning.

One-blade Constant Spinning[4]

Each plot in Fig. 2 shows only half of the system frequencies up to 3 Ω_0, i.e., positive frequencies, versus solar radiation pressure. The other half for the negative frequencies is a mirror image of the figure for the positive frequencies. Each plot is labeled with the number of beam modes used for describing the blade vibrational motions, and corresponding system order used to solve for the system eigenvalues. The first three frequencies are for in-plane, out-of-plane, and twist modes, respectively. Divergence instability, which has system eigenvalues with positive and negative real values, occurs when the number of beam modes used for in-plane, out-of-plane, and twist is less than 15. In addition, the divergence instability takes place at a higher solar radiation pressure with the increasing number of beam modes. Note that the third frequency for the first twist vibrational mode moves closer to the first in-plane frequency when the number of beam modes increases. Flutter instability occurs when the number of beam modes is 16 and the solar radiation pressure is $45 \times 10^{-6} N/m^2$. The first in-plane mode and the first twist mode have coalesced into two pairs of complex and conjugate modes (one pair has positive real parts and the other pair has negative real parts). Recall that for a stable system without material damping, each vibrational mode is represented by a pair of positive and negative pure imaginary values. For the case with 20 beam mode shapes, the flutter instability occurs at $\lambda = (\pm 0.04 \pm i0.67)$ with the solar radiation pressure at $41 \times 10^{-6} N/m^2$ (0.47 AU). The result shown in Fig. 2 is consistent with the study by Gibbs and Dowell.[9]

Three-blade Free Spinning

Figure 3 shows the frequencies versus radiation pressure for three-blade free spinning at 1 RPM with the blade locations at $(0^o, 120^o, 240^o)$ on a flat surface. In the absence of solar radiation pressure, the first 6 frequencies include 3 zero frequencies for translational motion, one zero frequency

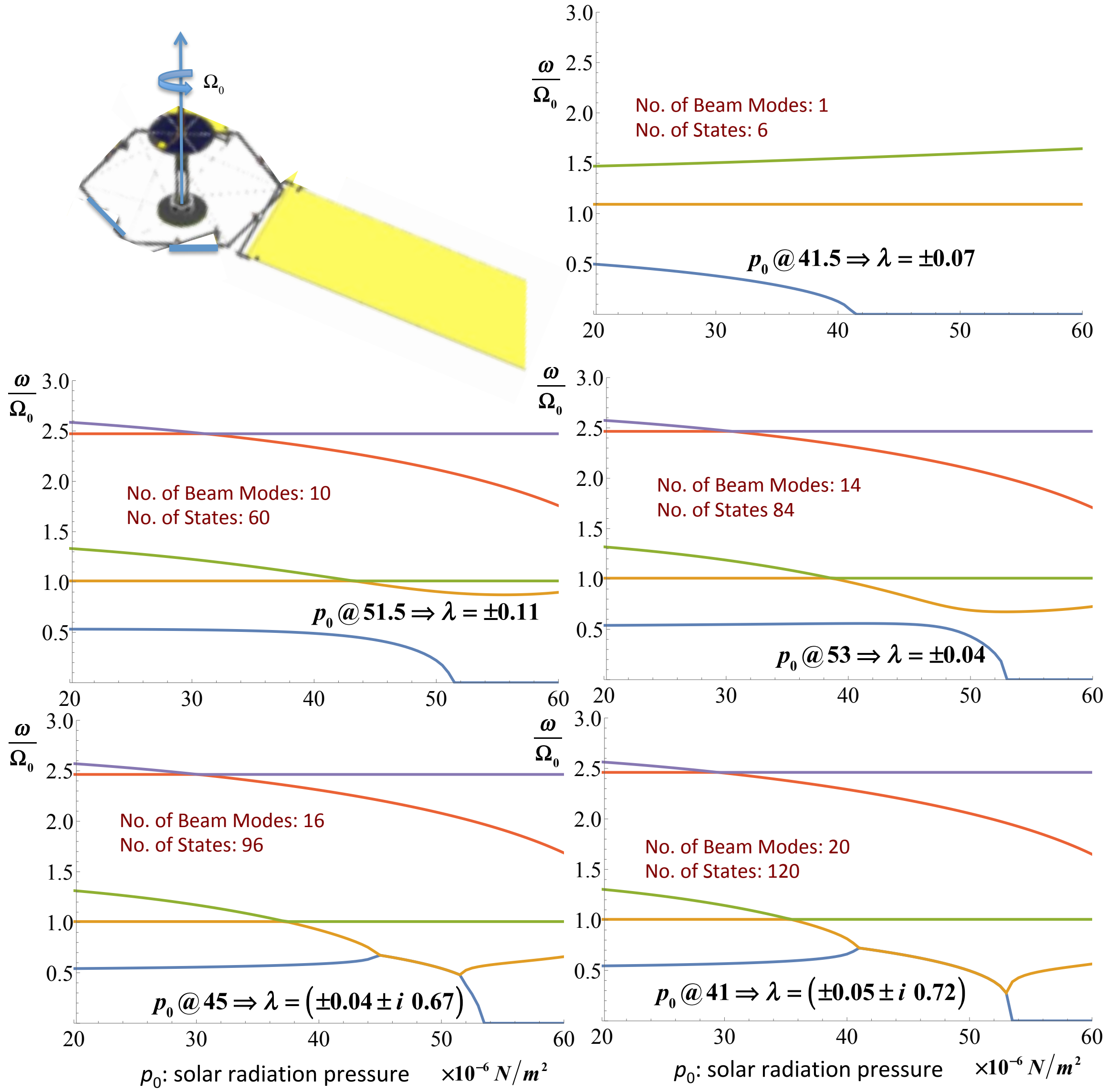

Figure 2. Normalized modal frequencies of a constant spinning heliogyro blade at 1RPM

for the spinning axis, and two nonzero frequencies for the other two hub rotational axes. For the case with solar radiation pressure at $p_0 = 35 \times 10^{-6} N/m^2$, the first nonzero frequency is 0.2Ω rad/sec which arises from the nonlinear second-order term associated with the centrifugal force due to the blade deflection. This nonlinear coupling also introduces a few dominant terms in the gyroscopic matrix at the degrees-of-freedom related to the spinning and blade vibrational states. With 1 beam mode for each blade vibrational motion (in-plane, out-of-plane, or twist), a flutter instability occurs when the spin frequency coalesced with the first in-plane blade mode at $p_0 = 36 \times 10^{-6} N/m^2$ and $\lambda = \pm 0.03 \pm 0.19i$. To contrast with 14 beam modes, the second in-plane frequency and the first twist frequency produce a flutter instability at $p_0 = 41.5 \times 10^{-6} N/m^2$ and $\lambda = \pm 0.01 \pm 0.83i$.

When the number of beam modes is larger than 15, the results show that the flutter instability points are converging. With 20 beam modes, the first flutter instability takes place at $p_0 = 37 \times 10^{-6} N/m^2$ and $\lambda = \pm 0.04 \pm 0.86i$, which occurs when the second in-plane and the first twist blade mode frequencies coalesce. In addition, there are two flutter points at $p_0 = 40.5 \times 10^{-6} N/m^2$ at $\lambda = \pm 0.02 \pm 0.74$ and $\lambda = \pm 0.15 \pm 0.80i$, caused by the second in-plane and the first twist blade mode frequencies, and the first in-plane and the second twist blade mode frequencies, respectively.

Six-blade Free Spinning

Figure 4 shows the frequencies versus radiation pressure for a six-blade configuration free spinning at 1 RPM with the blade locations at $(0^o, 60^o, 120^o, 180^o, 240^o, 300^o)$. The stability results for the 6-blade case are similar to those for the 3-blade case, except for two special instances. In contrast to the constant-spin single blade cases where the first in-plane frequency is the lowest mode, no divergence instability takes place earlier than the flutter instability even with using only one beam mode shapes for the free-spin multi-mode case. A common feature for the multi-blade case is that the twist frequencies move downward in value when the solar radiation pressure increases. Using 16 beam modes, a twist mode frequency will decrease as the specific radiation pressure increases to meet an in-plane mode frequency and coalesce to form a flutter instability mode, before another in-plane frequency coalesces with the oscillatory frequency of the spinning axis.

For the case with 20 beam modes shown in Fig. 5, a flutter instability takes place at a much higher frequency. However, this high-frequency instability problem does not exist for the cases with the number of beam modes less than 20 with an exception at 15 modes. At this point, it is possible that the high-frequency instability issue is caused by the numerical error in the beam modes at high frequency.

Mathematical formulations derived in this paper are used to verify the relationship between the flutter/divergence eigenvalues and eigenvectors for all cases with the constant-spin single blade and free-spin multiple blades. The relationship of eigenvectors associated with the flutter stable and unstable conjugate eigenvalues λ and λ^* can be used to develop a simple mode tracking algorithm for sensitivity analyses.

In summary, the number of beam mode shapes used to compute blade displacements plays a major role in approximating the blade kinetic and strain energies for developing the second-order matrix equation of motion for the heliogyro stability analysis. In theory, accuracy of the mathematical model increases with an increased number of modes at the expense of numerical accuracy. In our case, the cantilevered beam mode shapes are chosen to satisfy the characteristic equation $\cos(\beta_n)\cosh(\beta_n) = -1$ for in-plane and out-of-plane vibrational motions. For the 20th frequency, it requires a working precision up to 40 in Mathematica to satisfy the characteristic equation with

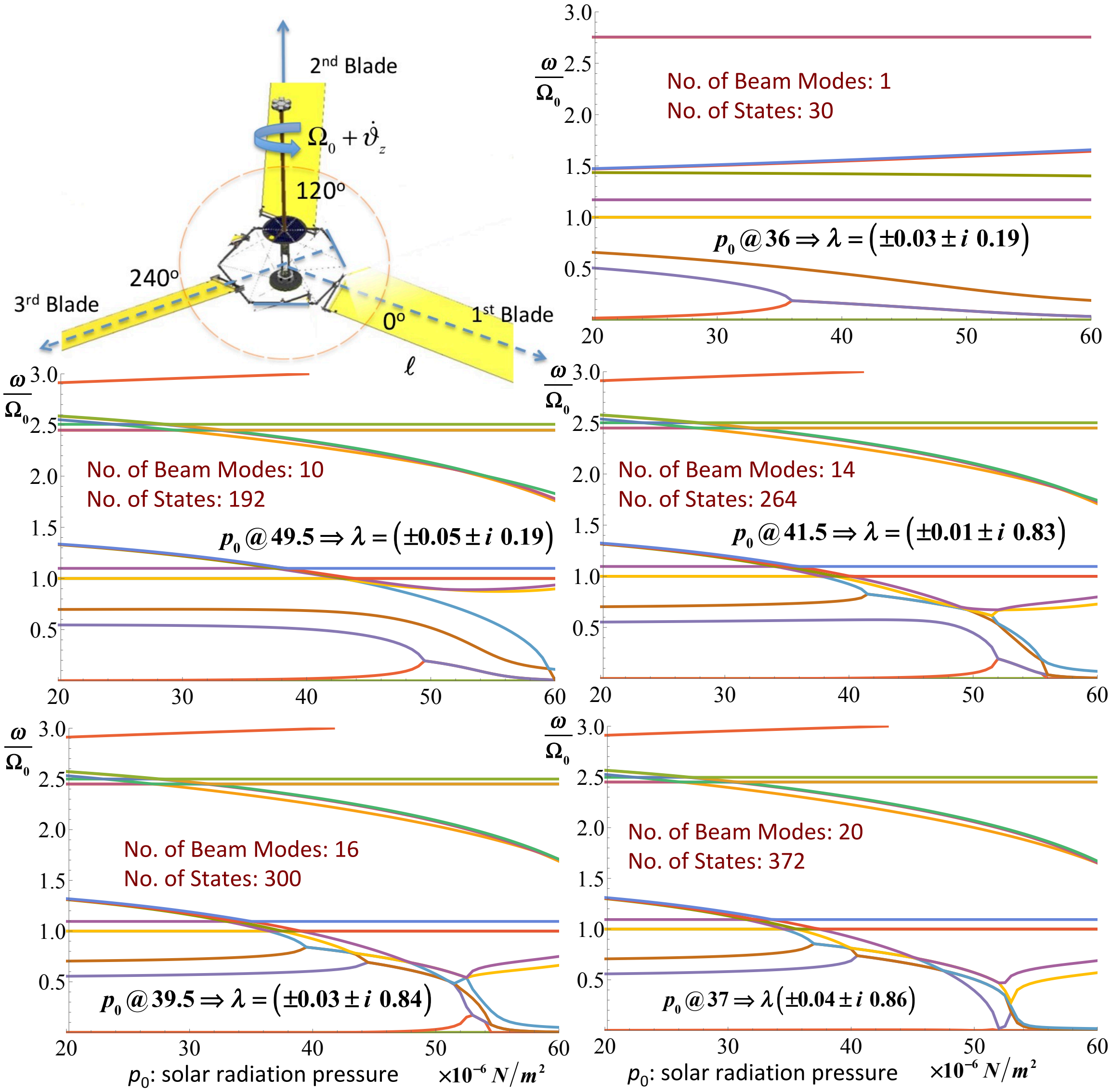

Figure 3. Normalized modal frequencies of three-heliogyro-blade free spinning at 1 RPM; locations of blades $(0^o, 120^o, 240^o)$

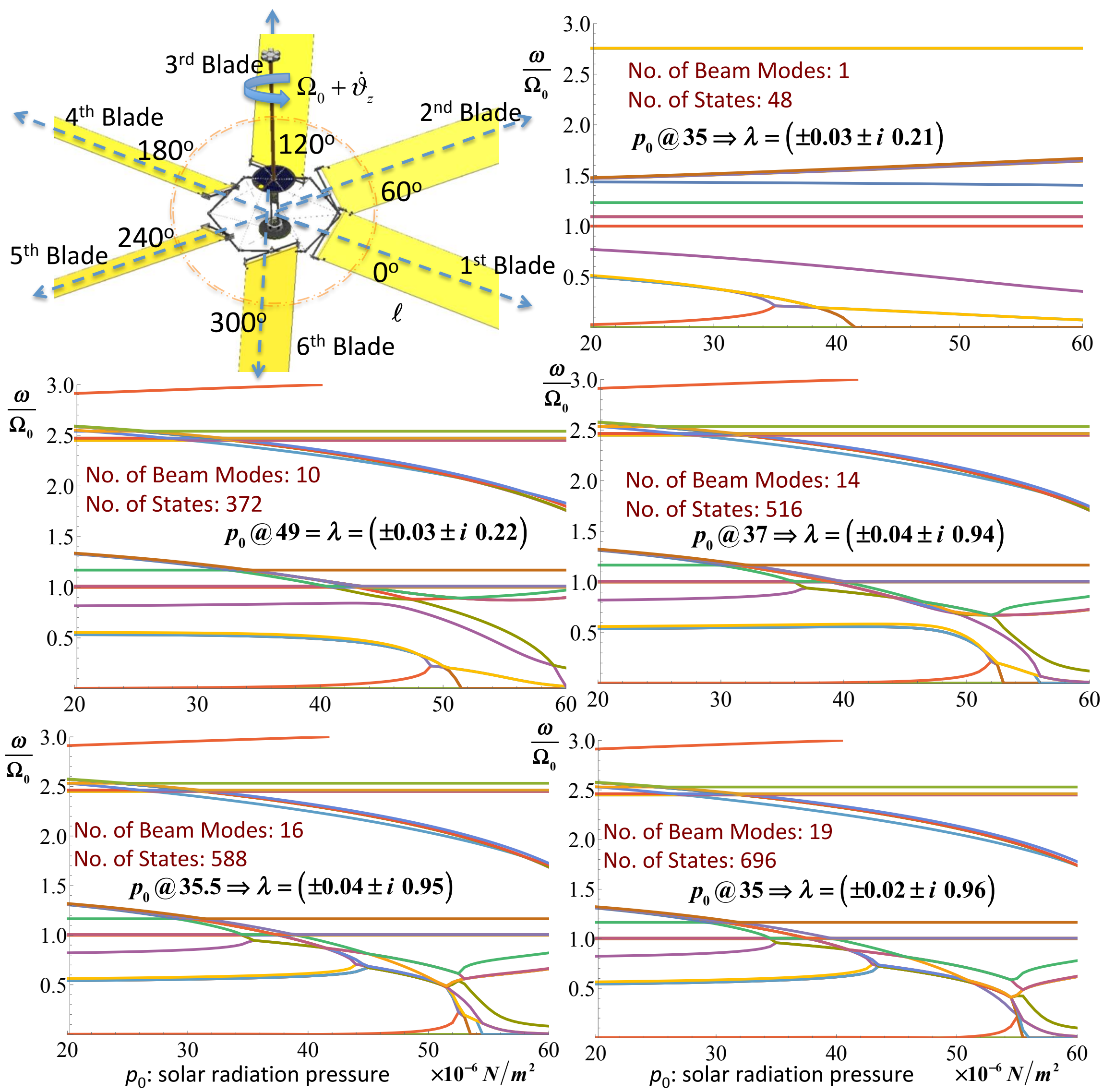

Figure 4. Normalized modal frequencies of six-heliogyro-blade free spinning at 1 RPM; locations of blades $(0^o, 60^o, 120^o, 180^o, 240^o, 300^o)$

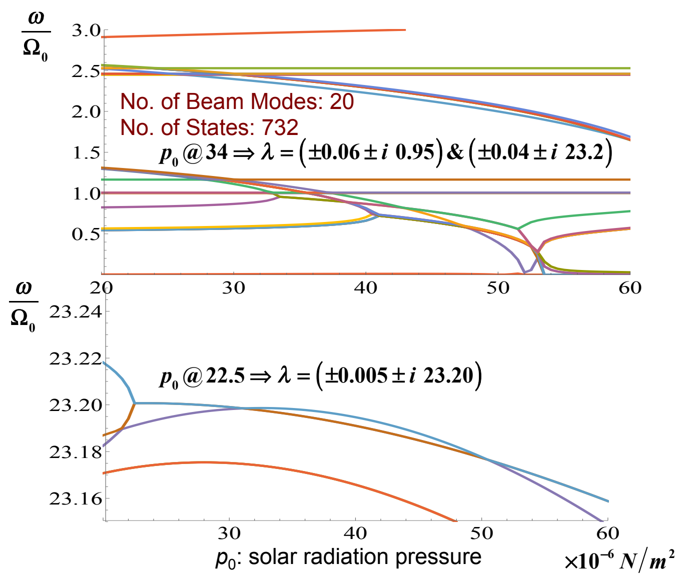

Figure 5. A singular case for six-blade free spinning at 1 RPM; locations of blades $(0^o, 60^o, 120^o, 180^o, 240^o, 300^o)$

10-digit accuracy. The size of the state matrix for stability analysis is 732×732 with 20 beam modes for each of the 3-direction blade displacements of a six-blade free-spinning heliogyro configuration as shown in Fig. 1. Use of Legendre functions, instead of cantilever beam mode shapes, was also examined, although system frequency convergence did not improve. Note that the Legendre functions do work well for membrane vibrational equations of motion. In addition, Dowell[20] presented a method for asymptotic approximations to beam mode shapes. For comparison, the modes from 5th to 20th were replaced by the approximated mode shapes for the case of six-blade free spinning at 1 RPM. The results are extremely close, if not identical, to the results shown in Figs. 4 and 5.

CONCLUSION

A free-spinning nonlinear heliogyro dynamic model for multiple blades attached to a rigid hub was developed for solarelastic stability analyses. The linearized second order heliogyro dynamic model developed here with respect to the static deflection relates the system eigenvalues and eigenvectors to solar radiation pressure and the flutter instability frequency. It was found that solarelastic flutter instabilities can only occur when the symmetry of the stiffness matrix is broken by the inclusion of solar radiation pressure and the induced static deflections of the blades. The solar radiation pressure also produces a small linear term for one-way coupling from twist to in-plane motion. Although the one-way coupling term is small relative other symmetric terms, it is sufficient to produce a flutter instability. Radiation pressure induced static deflections also change the symmetry of the mass matrix and the anti-symmetry of the gyroscopic matrix through the nonlinear terms. Nonetheless, these coupling terms are somewhat insignificant in comparison with other linear terms.

Coupling between twist and in-plane motions due to solar radiation pressure causes a solarelastic flutter instability. For the single-blade constant spinning case, flutter instability does not occur until the number of beam modes is greater than 15. For the 3-blade free-spinning case, flutter instability occurs when the second in-plane and first twisting vibrational modes coalesce into a complex mode with positive damping. This occurs when the number of beam modes $n \geq 14$. Similarly for the

6-blade free-spinning case, the flutter instability due to the coupling of in-plane and twist vibrational motions does not occur until the number of beam modes $n \geq 14$.

It has been established that a free-spinning stabilized satellite such as RAE/B subject to a conservative external force (i.e., gravitational force) may have divergence instability but not flutter instability, because the conservative force does not destroy the nature of the system matrices, i.e., the symmetry of the mass and stiffness matrices, and the antisymmetry of the gyroscopic matrix. In contrast to RAE, the free-spinning heliogyro may have flutter and/or divergence instabilities due to the presence of a non-conservative force (solar radiation pressure) that provides one-way coupling from twist to in-plane motions such that the symmetry of the stiffness matrix is no longer preserved.

ACKNOWLEDGEMENT

This work was sponsored in part under contract (Sub-award Number C17-2B53-JJ) from the National Aeronautics and Space Administration.

REFERENCES

[1] MacNeal, R. H., The Heliogyro: An Interplanetary Flying Machine, NASA Contractor Report CR 84460, June, 1967.

[2] MacNeal, R., H. Hedgepeth, J., Helicopters for Interplanetary Space Flight, 34th National Forum of the American Helicopter Society, Washington, D. C., May, 1978.

[3] Hodges, D. H., and Dowell, E. H. (1974) Nonlinear Equations of Motion for the Elastic Bending and Torsion of Twisted Nonuniform Rotor Blades, NASA TN D-7818, 1974.

[4] Juang, J.-N., Warren, J. E., Horta, L. G., Wilkie, W. K. Progress in NASA Heliogyro Solar Sail Structural Dynamics and Solarelastic Stability Research, The Fourth International Symposium on Solar Sailing, 17th-20th January, Kyoto Research Park, Kyoto, Japan, 2017.

[5] Wilkie, W. K., Warren, J. E., Horta, L.G., Lyle, K. H., Juang, J.-N., Gibbs, S. C., Dowell, E. H., Guerrant, D. V., Lawrence, D. A. (2015) Recent Advances in Heliogyro Solar Sail Structural Dynamics, Stability, and Control Research, AIAA SciTech 2015, Kissimee, Florida, January, 2015.

[6] Wilkie, W. K., Warren, J. E., Horta, L. G., Juang, J.-N., Gibbs, S. C., Dowell, E. H., Guerrant, D. V., Lawrence, D. A., Recent Progress in Heliogyro Solar Sail Structural Dynamics, presented at the European Conference on Spacecraft Structures, Materials, and Environmental Testing, Braunschweig, Germany, April 1-4, 2014, 2014

[7] Wilkie, W. K., Warren, J. E., Juang, J.-N., Horta, L. G., Lyle, K. H., Littell, J. D.,Bryant, R., G., Thomson, M. W., Walkemeyer, P. E., Guerrant, D. V., Lawrence, D. A., Gibbs, S. C., Dowell, E. H., and Heaton, A. F., Heliogyro Solar Sail Research at NASA, in: Macdonald, M. (Ed.), Advances in Solar Sailing, pp. 631-650, Springer-Praxis, Springer Berlin Heidelberg, 2014.

[8] Juang, J.-N., Hung, C.-H., and Wilkie, W. K., Dynamics of a Spinning Membrane, *The Journal of the Astronautical Sciences*, Published online: 30 October 2015, DOI 10.1007/s40295-015-0062-0 , Volume 60, No. 3-4, Dec. 2013, pp. 494?516; Special Issue: the Jer-Nan Juang Astrodynamics Symposium.

[9] Gibbs, S. C., Dowell, E. H., Solarelastic Stability of the Heliogyro, in: Macdonald, M. (Ed.), Advances in Solar Sailing, pp. 661-665, Springer-Praxis, Springer Berlin Heidelberg, 2014.

[10] Dowell, E. H., Can Solar Sails Flutter, *AIAA Journal*, Vol. 49, 1305-1307, 2011.

[11] Meirovitch, L. and Juang, J.-N., Dynamics of a Gravity-Gradient Stabilized Flexible Spacecraft, NASA Contrator Report for Research Grant NGR 47- 004-098, NASA CR-2456, August 1974

[12] Meirovitch, L. and Juang, J.-N., On the Natural Modes of Oscillation of Rotating Flexible Structure about Nontrivial Equilibrium, *Journal of Spacecraft and Rockets*, Vol. 13, Jan. 1976, pp. 33-44.

[13] Meirovitch, L. and Juang, J.-N., Effect of the Mass Center Shift for Force-Free Flexible Spacecraft, *AIAA Journal*, Vol.13, Nov. 1975, pp. 1535-1536.

[14] Meirovitch, L., Hybrid State Equations of Motion for Flexible Bodies in Terms of Quasi-Coordinates, *Journal of Guidance, Dynamics, and Control*, Vol.14, Sept.-Oct. 1991, pp. 1008-1013.

[15] Lee, S. and Junkins, J. L., Explicit Generalization of Lagrange's Equations for Hybrid Coordinate Dynamical Systems, *Journal of Guidance, Dynamics, and Control*, Vol.15, No. 6, November-December 1992, pp. 1443-1452.

[16] Junkins, J. L. and Kim, Y., Introduction to Dynamics and Control of Flexible Structures, American Institute of Aeronautics and Astronautics, Washington, DC, 1993, 452 pp.

[17] Natori, M., Nemat-Nasser, S., Mitsugi, J. (1989) Instability of a Rotating Blade Subjected to Solar Radiation Pressure, AIAA 30th Structures, Structural Dynamics and Materials Conference, 1989.

[18] Natori, M. and Nenat-Nasser, S. (1986) Application of a Mixed Variational Approach to Aeroelastic Stability Analysis of a Nonuniform Blade,*Journal of Structural Mechanics*, Vo1. l4, pp. 5-31, 1986.

[19] Gibbs, S.C., and Dowell, E.H., Membrane paradox for solar sails. AIAA Journal, Vol. 52, pp. 2904-2906, 2014.

[20] Dowell, E.H., On asymptotic approximations to beam mode shapes. Journal of Applied Mechanics, Vol. 5, No. 12, page 439, 1984.

NOMENCLATURE

$\bar{I}_{xx}, \bar{I}_{yy}, \bar{I}_{zz}$	$\bar{I}_{xx} = I_{xx}/m_b\ell^2, \bar{I}_{yy} = I_{yy}/m_b\ell^2, \bar{I}_{zz} = I_{zz}/m_b\ell^2$
ℓ	blade length
ν	poison ratio
Ω_0	nominal spin rate of heliogyro, rad/sec
$\overline{p}$	non-dimensional p_0; $\overline{p} = (p_0 c)/(m_b\Omega_0^2)$
$\overline{R}_x, \overline{R}_y, \overline{R}_z$	$\overline{R}_x = R_x/\ell, \overline{R}_y = R_y/\ell, \overline{R}_z = R_z/\ell$
$\overline{u}_k, \overline{v}_k, \overline{w}_k$	$\overline{u}_k = u_k/\ell, \overline{v}_k = v_k/\ell, \overline{w}_k = w_k/\ell$
ρ	density per unit volume for blades; kg/m^3
$\mathbf{e}_{hx}, \mathbf{e}_{hy}, \mathbf{e}_{hz}$	orthogonal unit vectors of the hub frame
$\mathbf{e}_{Ix}, \mathbf{e}_{Iy}, \mathbf{e}_{Iz}$	orthogonal unit vectors of the inertia frame
$\mathbf{e}_{kx}, \mathbf{e}_{k\eta}, \mathbf{e}_{k\zeta}$	orthogonal unit vectors of the kth blade frame
$\varphi_{u_k i}, \varphi_{v_k i}, \varphi_{w_K i}, \varphi_{\phi_k i}$	ith mode shape for elastic displacements of the kth blade
$\vartheta_x, \vartheta_y, \vartheta_z$	rotational angles of the hub frame
c	blade width
E	Young$'$s modulus
G	torsional rigidity; $G \approx E/[2(1+)\nu]$
i, j, k	integers for indexing mode shapes
I_{xx}, I_{yy}, I_{zz}	hub moment of inertia
m, m_b	blade density per unit length (kg/m), total mass of a blade ($m_b = m\ell$ for a constant m)
$m_h, \bar{m}_h$	hub mass (kg), $\bar{m}_h = m_h/m_b$
p_0	solar radiation pressure; N/m^2
R_x, R_y, R_z	translational displacements of the hub frame
u'_k, v'_k, w'_k	$u'_k = \partial u_k/\partial x, v'_k = \partial v_k/\partial x, w'_k = \partial w_k/\partial x$

v_k, w_k, u_k, ϕ_k	In-plane, out-of-plane, elongation elastic displacements, and twist angle of the kth blade
x, y, z	hub coordinates along the principal axes
x_k, ξ_k, η_k	blade coordinates of the kth blade

APPENDIX A: ORDER OF VARIABLES

The equations of motion for the heliogyro system with multiple blades are expected to be highly nonlinear. It is necessary to neglect higher-order terms for stability analysis. The following is a list of non-dimensional variables of order[3] for use in deriving blade strain energy and system kinetic energy to generate the dynamic equations using Hamilton's principle. This list is applicable for any number of blades with equal length and so no subscript such as k for any designated blade is shown.

$$\frac{\zeta}{\ell} = \mathrm{O}(\varepsilon); \quad \frac{\eta}{\ell} = \mathrm{O}(\varepsilon); \quad \xi = \frac{x}{\ell} = \mathrm{O}(1)$$

$$\bar{v} = \frac{v}{\ell} = \mathrm{O}(\varepsilon); \quad v' = \frac{\partial(v/\ell)}{\partial(x/\ell)} = \bar{v}' = \mathrm{O}(\varepsilon); \quad v'' = \frac{1}{\ell}\frac{\partial^2(v/\ell)}{\partial\left(x^2/\ell^2\right)} = \frac{1}{\ell}\bar{v}'' = \mathrm{O}\left(\varepsilon^2\right)$$

$$\bar{w} = \frac{w}{\ell} = \mathrm{O}(\varepsilon); \quad w' = \frac{\partial(w/\ell)}{\partial(x/\ell)} = \bar{w}' = \mathrm{O}(\varepsilon); \quad w'' = \frac{1}{\ell}\frac{\partial^2(w/L)}{\partial\left(x^2/L^2\right)} = \frac{1}{\ell}\bar{w}'' = \mathrm{O}\left(\varepsilon^2\right)$$

$$\phi = \mathrm{O}(\varepsilon); \quad \phi' = \frac{1}{\ell}\frac{\partial\phi}{\partial(x/\ell)} = \frac{1}{\ell}\bar{\phi}' = \mathrm{O}\left(\varepsilon^2\right);$$

APPENDIX B: DEFINITIONS OF SECTIONAL INTEGRALS

Assume that all blades have identical material properties and configuration. The sectional integrals are shown in the following.[3]

$$\int\int_A \rho d\eta d\zeta = m = \rho A \text{ (for constant } \rho \text{ and } A)$$

$$\int\int_A \rho\eta d\eta d\zeta = 0; \int\int_A \rho\zeta d\eta d\zeta = 0$$

$$\int\int_A \rho\eta^2 d\eta d\zeta = mk_{m2}^2; \int\int_A \rho\zeta^2 d\eta d\zeta = mk_{m1}^2$$

$$\int\int_A \rho\left[\eta - \zeta\right]\left[\eta + \zeta\right] d\eta d\zeta = m\left(k_{m2}^2 - k_{m1}^2\right) = m\Delta k_m^2$$

$$\int\int_A \rho\left(\eta^2 + \zeta^2\right) d\eta d\zeta = m\left(k_{m2}^2 + k_{m1}^2\right) = mk_m^2$$

$$I_v = \int\int_A \eta^2 d\eta d\zeta; I_w == \int\int_A \zeta^2 d\eta d\zeta; Ak_a^2 = \int\int_A \left(\eta^2 + \zeta^2\right) d\eta d\zeta$$

$$A = \int\int_A d\eta d\zeta; \int\int_A \zeta d\eta d\zeta = 0; \int\int_A \eta\zeta d\eta d\zeta = 0; J \approx 4I_w$$

APPENDIX C: DEFINITION OF NON-DIMENSIONAL PARAMETERS

It is a common practice to use non-dimensional parameters to develop equations of motion.[3] Dimensionless analysis is often used to generalize the problem, because solution of dimensional form is the solution of a particular problem. Non-dimensional equations will reduce the number of variables and provide insight into the controlling parameters. Non-dimensional parameters used in the paper are given as follows.

$$\xi=\frac{x}{\ell};\dot{\bar{\vartheta}}_x=\frac{\dot{\vartheta}_x}{\Omega_0};\ddot{\bar{\vartheta}}_x=\frac{\ddot{\vartheta}_x}{\Omega_0^2};\dot{\bar{\vartheta}}_y=\frac{\dot{\vartheta}_y}{\Omega_0};\dot{\bar{\vartheta}}_y=\frac{\ddot{\vartheta}_y}{\Omega_0^2};\dot{\bar{\vartheta}}_z=\frac{\dot{\vartheta}_z}{\Omega_0};\ddot{\bar{\vartheta}}_z=\frac{\ddot{\vartheta}_z}{\Omega_0^2}$$

$$\bar{T}=\frac{T}{m\Omega_0^2\ell^2};\bar{G}\bar{J}=\frac{GJ}{m\Omega_0^2\ell^4};\bar{E}\bar{I}_w=\frac{EI_w}{m\Omega_0^2\ell^4};\bar{E}\bar{I}_v=\frac{EI_2}{m\Omega_0^2\ell^4};\Delta\bar{E}\bar{I}=\bar{E}\bar{I}_v-\bar{E}\bar{I}_w$$

$$\bar{u}=\frac{u}{\ell},\bar{v}=\frac{v}{\ell},\bar{w}=\frac{w}{\ell}:\tau=\Omega_0 t\Rightarrow\frac{\partial()}{\partial t}=\frac{\Omega_0\partial()}{\partial\tau};\frac{\partial\phi}{\partial\xi}=\frac{\partial\phi}{\partial(x/\ell)}=\frac{\ell\partial\phi}{\partial x}$$

$$\bar{v}'=\frac{\partial\bar{v}}{\partial\xi}=\frac{\partial(v/\ell)}{\partial(x/\ell)}=v';\bar{v}''=\frac{\partial^2(v/\ell)}{\partial\left(x^2/\ell^2\right)}=\ell v'';\ddot{\bar{v}}'=\frac{d^2}{\Omega_0^2dt^2}\frac{\partial(v/\ell)}{\partial(x/\ell)}=\frac{1}{\Omega_0^2}\ddot{v}'$$

$$\bar{T}'=\frac{\partial\bar{T}}{\partial\xi}=\frac{\partial\bar{T}}{\partial(x/\ell)}=\frac{1}{m\Omega_0^2\ell}\frac{\partial T}{\partial x};\frac{d\bar{v}}{d\tau}=\frac{d(v/\ell)}{d\Omega_0 t}=\frac{1}{\ell\Omega_0}\frac{dv}{dt}\Rightarrow\frac{\Omega_0\dot{v}}{\ell^2\Omega_0^2}=\frac{\ell\Omega_0^2\dot{\bar{v}}}{\ell^2\Omega_0^2}\Rightarrow\frac{\dot{\bar{v}}}{\ell}$$

$$\bar{k}_m=\frac{k_m}{\ell},\bar{k}_{m_1}=\frac{k_{m_1}}{\ell},\bar{k}_{m_2}=\frac{k_{m_2}}{\ell}$$

APPENDIX D: EQUATIONS OF MOTION FROM KINETIC AND STRAIN ENERGIES

The kinetic energy for the kth blade can be calculated by

$$\mathcal{T}_k=\frac{1}{2}\int_0^{\ell_k}\int\int_A\rho_k\dot{\mathbf{r}}_k\cdot\dot{\mathbf{r}}_k d\zeta_k d\eta_k dx_k \tag{D1}$$

where the position **r** is defined in Eq. (2). The ratio $H_{kx}/\ell << 1$ is very small, i.e., the distance from the center of hub to the root of the k blade is negligible compared to the blade length. Taking variation of the kinetic energy and integrating from t_0 to t_f yield

$$\int_{t_0}^{t_f}\delta T_k dt=\int_{t_0}^{t_f}\int_0^{\ell_k}\int\int_A\rho_k\dot{\mathbf{r}}_k\cdot\delta\dot{\mathbf{r}}_k d\zeta_k d\eta_k dx_k dt \tag{D2}$$

Using the non-dimensional parameters defined in Appendix C, the non-dimensional variation of kinetic energy for the kth blade is

$$\int_{\tau_0}^{\tau}\delta\bar{\mathcal{T}}_k d\tau=-\int_{\tau_0}^{\tau}\left[\delta q^T\int_0^1\left(\hat{M}_k\ddot{q}+\hat{C}_k\dot{q}+\hat{K}_k q\right)d\xi_k-\sum_{i=1}^{n}\int_0^1\varphi_{u_k i}\xi_k d\xi_k\delta q_{u_i k}\right]d\tau \tag{D3}$$

where the generalized coordinate vector is

$$q=\left[\begin{array}{cccccccccc}\bar{R}_x & \bar{R}_y & \bar{R}_z & \bar{\vartheta}_x & \bar{\vartheta}_y & \bar{\vartheta}_z & q_{w_k i} & q_{v_k i} & q_{\phi_k i} & q_{u_k i}\end{array}\right]^T$$

and the shape functions are defined in Eq. (4), i.e., $\varphi_{w_k i}$, $\varphi_{v_k i}$, $\varphi_{u_\phi i}$, for $i=1,2,\ldots,n$. The mass matrix $\hat{M}_k$, the gyroscopic $\hat{C}_k$, and the stiffness matrix $\hat{K}_k$ due to the spinning Ω_0 are given as follows.

Mass Matrix from Variation of Kinetic Energy

The mass matrix for the kth blade from the variation of kinetic energy is

$$\bar{M}_k=\int_0^1\hat{M}_k d\xi_k;\quad\hat{M}_k=\left[\begin{array}{cc}\hat{M}_{k_{RR}} & \hat{M}_{k_{RB}}\\ \hat{M}_{k_{RB}}^T & \hat{M}_{k_{BB}}\end{array}\right] \tag{D4}$$

where the 6×6 submatrix $\hat{M}_{k_{RR}}$ gives the coupling between the hub translational and rotational coordinates,

$$\hat{M}_{k_{RR}} = \begin{pmatrix} 1 & 0 & 0 & 0 & 0 & \xi_k s\theta_k \\ 0 & 1 & 0 & 0 & 0 & \xi_k c\theta_k \\ 0 & 0 & 1 & -\xi_k s\theta_k & -\xi_k c\theta_k & 0 \\ 0 & 0 & -\xi_k s\theta_k & \bar{k}_{m1}^2 + \bar{k}_{m2}^2 c^2\theta_k + \xi_k^2 \mathrm{s}^2\theta_k & \left(\xi_k^2 - \bar{k}_{m2}^2\right) c\theta_k s\theta_k & 0 \\ 0 & 0 & -\xi_k c\theta_k & \left(\xi_k^2 - \bar{k}_{m2}^2\right) c\theta_k s\theta_k & \begin{matrix} \bar{k}_{m1}^2 + \xi_k^2 c^2\theta_k \\ +\bar{k}_{m2}^2 s^2\theta_k \end{matrix} & 0 \\ \xi_k s\theta_k & \xi_k c\theta_k & 0 & 0 & 0 & \bar{k}_{m2}^2 + \xi_k^2 \end{pmatrix} \quad \text{(D5)}$$

the $6 \times 4n$ rectangular matrix $\hat{M}_{k_{RB}}$ shows the coupling of the translational and rotational coordinates with the blade vibrational generalized coordinates,

$$\hat{M}_{k_{RB}} = \begin{pmatrix} 0 & \varphi_{v_k j} s\theta_k & 0 & \varphi_{u_k j} c\theta_k \\ 0 & \varphi_{v_k j} c\theta_k & 0 & -\varphi_{u_k j} s\theta_k \\ \varphi_{w_k j} & 0 & 0 & 0 \\ -s\theta_k \left(\varphi_{w_k j}' \bar{k}_{m1}^2 + \xi \varphi_{w_k j}\right) & 0 & k_m^2 \varphi_{\phi_k j} c\theta_k & 0 \\ -c\theta_k \left(\varphi_{w_k j}' \bar{k}_{m1}^2 + \xi \varphi_{w_k j}\right) & 0 & -k_m^2 \varphi_{\phi_k j} s\theta_k & 0 \\ 0 & \left(\varphi_{v_k j}' \bar{k}_{m2}^2 + \xi \varphi_{v_k j}\right) & 0 & 0 \end{pmatrix} \quad \text{(D6)}$$

and the $4n \times 4n$ matrix $\hat{M}_{k_{BB}}$ is associated with the blade vibrational generalized coordinates

$$\hat{M}_{k_{BB}} = \begin{pmatrix} \varphi_{w_k i}\varphi_{w_k j} + \bar{k}_{m1}^2 \varphi_{w_k i}' \varphi_{w_k j}' & 0 & 0 & 0 \\ 0 & \varphi_{v_k i}\varphi_{v_k j} + \bar{k}_{m2}^2 \varphi_{v_k i}' \varphi_{v_k j}' & 0 & 0 \\ 0 & 0 & \bar{k}_m^2 \varphi_{\phi_k i}\varphi_{\phi_k j} & 0 \\ 0 & 0 & 0 & \varphi_{u_k i}\varphi_{u_k j} \end{pmatrix} \quad \text{(D7)}$$

with

$$s\theta_k = \sin\theta_k; c\theta_k = \cos\theta_k$$

Note that the mass matrix is symmetric such that $\bar{M}_k = \bar{M}_k^T$ and positive definite $\bar{M} > 0$.

Gyroscopic Matrix from Variation of Kinetic Energy

The gyroscopic matrix for the kth blade from the variation of kinetic energy is

$$\bar{C}_k = \int_0^1 \hat{C} d\xi; \quad \hat{C}_k = \begin{bmatrix} \hat{C}_{k_{RR}} & \hat{C}_{k_{RB}} \\ -\hat{C}_{k_{RB}}^T & \hat{C}_{k_{BB}} \end{bmatrix} \quad \text{(D8)}$$

where the 6×6 matrix $\hat{C}_{k_{RR}}$ is a skew symmetric matrix,

$$\hat{C}_{k_{RR}} = \begin{pmatrix} 0 & 0 & 0 & 0 & 0 & -\xi_k c\theta_k \\ 0 & 0 & 0 & 0 & 0 & \xi_k s\theta_k \\ 0 & 0 & 0 & 0 & 0 & 0 \\ 0 & 0 & 0 & 0 & -2\bar{k}_{m1}^2 & 0 \\ 0 & 0 & 0 & 2\bar{k}_{m1}^2 & 0 & 0 \\ \xi_k c\theta_k & -\xi_k s\theta_k & 0 & 0 & 0 & 0 \end{pmatrix} \quad \text{(D9)}$$

and the $6 \times 4n$ rectangular matrix $\hat{C}_{k_{RB}}$ is

$$\hat{C}_{k_{RB}} = \begin{pmatrix} 0 & -\varphi_{v_kj} c\theta_k & 0 & \varphi_{u_kj} s\theta_k \\ 0 & \varphi_{v_kj} s\theta_k & 0 & \varphi_{u_kj} c\theta_k \\ 0 & 0 & 0 & 0 \\ 2\bar{k}_{m1}^2 \varphi'_{w_kj} c\theta_k & 0 & 2\bar{k}_{m1}^2 \varphi_{\phi_kj} s\theta_k & 0 \\ -2\bar{k}_{m1}^2 \varphi'_{w_kj} s\theta_k & 0 & 2\bar{k}_{m1}^2 \varphi_{\phi_kj} c\theta_k & 0 \\ 0 & 0 & 0 & 2\varphi_{u_kj} \xi_k \end{pmatrix} \tag{D10}$$

and the $4n \times 4n$ matrix $\hat{C}_{k_{BB}} = -\hat{C}_{k_{BB}}^T$ is

$$\hat{C}_{k_{BB}} = \begin{pmatrix} 0 & 0 & -2\bar{k}_{m1}^2 \varphi_{\phi_kj} \varphi'_{w_ki} & 0 \\ 0 & 0 & 0 & 2\varphi_{u_kj} \varphi_{v_ki} \\ 2k_{m1}^2 \varphi_{\phi_ki} \varphi'_{w_kj} & 0 & 0 & 0 \\ 0 & -2\varphi_{u_ki} \varphi_{v_kj} & 0 & 0 \end{pmatrix} \tag{D11}$$

Note that the gyroscopic matrix is skew symmetric such that $\bar{C}_k = -\bar{C}_k^T$.

Stiffness Matrix from Variation of Kinetic Energy for a Spinning System

The stiffness matrix for the kth blade subject to a nominal spinning rate Ω_0 is

$$\bar{K}_k = \int_0^1 \hat{K}_k d\xi; \quad \Delta\bar{k}_m^2 = \bar{k}_{m2}^2 - \bar{k}_{m1}^2; \quad \hat{K}_k = \begin{bmatrix} \hat{K}_{k_{RR}} & \hat{K}_{k_{RB}} \\ \hat{K}_{k_{RB}}^T & \hat{K}_{k_{BB}} \end{bmatrix} \tag{D12}$$

where the 6×6 matrix $\hat{K}_{k_{RR}}$ is symmetric,

$$\hat{K}_{k_{RR}} = \begin{pmatrix} 0 & 0 & 0 & 0 & 0 & 0 \\ 0 & 0 & 0 & 0 & 0 & 0 \\ 0 & 0 & 0 & 0 & 0 & 0 \\ 0 & 0 & 0 & \bar{k}_{m2}^2 c^2\theta_k - \bar{k}_{m1}^2 + \xi_k^2 s^2\theta_k & \left(\xi_k^2 - \bar{k}_{m2}^2\right) c\theta_k s\theta_k & 0 \\ 0 & 0 & 0 & \left(\xi_k^2 - \bar{k}_{m2}^2\right) c\theta_k s\theta_k & \xi_k^2 c^2\theta_k - \bar{k}_{m1}^2 + \bar{k}_{m2}^2 s^2\theta_k & 0 \\ 0 & 0 & 0 & 0 & 0 & 0 \end{pmatrix} \tag{D13}$$

and the $6 \times 4n$ rectangular matrix $\hat{K}_{k_{RB}}$ is

$$\hat{K}_{k_{RB}} = \begin{pmatrix} 0 & 0 & 0 & 0 \\ 0 & 0 & 0 & 0 \\ 0 & 0 & 0 & 0 \\ \left(\bar{k}_{m1}^2 \varphi'_{w_kj} - \xi\varphi_{w_kj}\right) s\theta_k & 0 & \varphi_{\phi_kj} \Delta\bar{k}_m^2 c\theta_k & 0 \\ \left(\bar{k}_{m1}^2 \varphi'_{wj} - \xi\varphi_{wj}\right) c\theta_k & 0 & -\varphi_{\phi j} \Delta\bar{k}_m^2 s\theta_k & 0 \\ 0 & 0 & 0 & 0 \end{pmatrix} \tag{D14}$$

and the $4n \times 4n$ matrix $\hat{K}_{BB} = \hat{K}_{k_{BB}}^T$ is

$$\hat{K}_{k_{BB}} = \begin{pmatrix} -\bar{k}_{m1}^2 \varphi'_{wi} \varphi'_{wj} & 0 & 0 & 0 \\ 0 & \left(-\varphi_{vi}\varphi_{vj} - \bar{k}_{m2}^2 \varphi'_{vi} \varphi'_{vj}\right) & 0 & 0 \\ 0 & 0 & \varphi_{\phi i} \varphi_{\phi j} \Delta\bar{k}_m^2 & 0 \\ 0 & 0 & 0 & -\varphi_{ui}\varphi_{uj} \end{pmatrix} \tag{D15}$$

Note that the stiffness matrix from the variation of kinetic energy is symmetric, i.e., $\bar{K}_k = \bar{K}_k^T$ but may not be positive definite.

There is a single variation term shown in Eq. (D3) associated with the blade elongation displacement, i.e.,

$$-\int_0^1 \varphi_{u_k i}\xi_k \delta q_{u_i k} d\xi_k \tag{D16}$$

This term results from the product of ξ_k and $\bar{u}_k$. It is an important term for solving the centrifugal force to be discussed later.

Stiffness Matrix from Variation of Strain Energy

The first variation of the strain energy for a blade in terms of engineering stresses and strains is

$$\delta\mathcal{V} = \frac{1}{2}\int_0^\ell \int\int_A \left(\sigma_{xx}\delta\varepsilon_{xx} + \sigma_{x\eta}\delta\varepsilon_{x\eta} + \sigma_{x\zeta}\delta\varepsilon_{x\zeta}\right) d\eta d\zeta dx \tag{D17}$$

where

$$\begin{aligned} \sigma_{xx} &= E\varepsilon_{xx} = E\left[\begin{array}{c} \frac{v'^2}{2} + \frac{w'^2}{2} + u' + \frac{\phi'^2}{2}\left(\eta^2+\zeta^2\right) \\ -\left(v''-w'\phi'\right)\left(\eta\cos\phi - \zeta\sin\phi\right) - \left(w''+v'\phi'\right)\left(\zeta\cos\phi + \eta\sin\phi\right) \end{array}\right] \\ \sigma_{x\eta} &= G\varepsilon_{x\eta} \\ \sigma_{x\zeta} &= G\varepsilon_{x\zeta} \end{aligned} \tag{D18}$$

and

$$\begin{aligned} \delta\varepsilon_{xx} &= \delta u' + v'\delta v' + w'\delta w' + \left(\eta^2+\zeta^2\right)\phi'\delta\phi' - \left[\eta\cos\phi - \zeta\sin\phi\right]\left(\delta v'' + w''\delta\phi\right) \\ &\quad - \left[\eta\sin\phi + \zeta\cos\phi\right]\left(\delta w'' + v''\delta\phi\right) \\ \delta\varepsilon_{x\eta} &= -\zeta\delta\phi' \\ \delta\varepsilon_{x\zeta} &= \eta\delta\phi' \end{aligned} \tag{D19}$$

where the terms $w'\phi'$ and $v'\phi'$ in Eq. (D18) are one order in magnitude smaller than the other terms in their respective parentheses and thus ignored in the following derivation. Nevertheless, it is still debatable that these ignored terms may have some non-negligible contributions to the stiffness matrix.

Define the quantity for the kth blade

$$T_k = EA\left(\frac{v'^2_k}{2} + \frac{w'^2_k}{2} + u'_k + k_A^2\frac{\phi'^2_k}{2}\right) \approx EA\left(\frac{v'^2_k}{2} + \frac{w'^2_k}{2} + u'_k\right) \tag{D20}$$

which is related to the centrifugal force for a spinning blade. The non-dimensional variation of the strain energy becomes

$$
\begin{aligned}
\delta\bar{\mathcal{V}} = &\sum_{k=1}^{n_b}\int_0^1 \left\{\left[\bar{E}\bar{I}_w\bar{w}_k'' + \Delta\bar{E}\bar{I}\phi_k\bar{v}_k''\right]\delta\bar{w}_k'' + \bar{T}_k\bar{w}_k'\delta\bar{w}_k' + \bar{E}\bar{I}_w\bar{\phi}_k'\bar{v}_k'\delta\bar{w}_k'' - \bar{E}\bar{I}_v\bar{\phi}_k'\bar{v}_k''\delta\bar{w}_k'\right\}d\xi_k \\
&+\sum_{k=1}^{n_b}\int_0^1 \left\{\left[\bar{E}\bar{I}_v\bar{v}_k'' + \Delta\bar{E}\bar{I}\phi\bar{w}_k''\right]\delta\bar{v}_k'' + \bar{T}_k\bar{v}'\delta\bar{v}_k' - \bar{E}\bar{I}_v\bar{\phi}_k'\bar{w}_k'\delta\bar{v}_k'' + \bar{E}\bar{I}_w\bar{\phi}_k'\bar{w}_k''\delta\bar{v}_k'\right\}d\xi_k \\
&+\sum_{k=1}^{n_b}\int_0^1 \left\{\left[\left(\bar{G}\bar{J} + \bar{T}_k\bar{k}_A^2\right)\phi_k'\right]\delta\phi_k' + \Delta\bar{E}\bar{I}\bar{v}_k''\bar{w}_k''\delta\phi_k - \bar{E}\bar{I}_v\bar{v}_k''\bar{w}_k'\delta\bar{\phi}_k' + \bar{E}\bar{I}_w\bar{v}_k'\bar{w}_k''\delta\bar{\phi}_k'\right\}d\xi_k \\
&+\sum_{k=1}^{n_b}\int_0^1 \bar{T}_k\delta u_k' d\xi
\end{aligned}
\tag{D21}
$$

Assume that all deflection quantities are function separable, substituting Eq. (5) into Eq. (D21) produces the non-dimensional variation of strain energy for the kth blade

$$
\delta\bar{\mathcal{V}}_k = \int_{\tau_0}^{\tau}\left[\delta q_b^T\bar{K}_{k_S}q_b + \sum_{i=1}^{n}\int_0^1 \bar{T}_k\varphi'_{u_k i}d\xi_k\delta q_{u_k i}\right]d\tau
$$

where $q_b = \begin{bmatrix} q_{w_k i} & q_{v_k i} & q_{\phi_k i} & q_{u_k i}\end{bmatrix}^T$ are the generalized coordinates associated with the strain energy. The $4n\times 4n$ stiffness matrix $\bar{K}_{k_S}$ associated with the generalized coordinates $(q_{w_k i}, q_{v_k i}, q_{\phi_k i}, q_{u_k i})$ for the k blade from the strain variation is

$$
\bar{K}_{k_S} = \int_0^1 \hat{K}_{k_S}d\xi_k; \Delta EI = \bar{E}\bar{I}_v - \bar{E}\bar{I}_w \tag{D22}
$$

$$
\hat{K}_{k_S} = \begin{bmatrix}
\begin{pmatrix}\bar{E}\bar{I}_w\varphi''_{w_k i}\varphi''_{w_k j} \\ +\bar{T}_k{\varphi'}_{w_k i}{\varphi'}_{w_k j}\end{pmatrix} & q_{\phi_k\gamma}\Delta EI\varphi_{\phi\gamma}\varphi''_{w_k i}\varphi''_{v_k j} & q_{v_k\gamma}\Delta EI\varphi''_{v_k\gamma}\varphi''_{w_k i}\varphi_{\phi_k j} & 0 \\
q_{\phi_k\gamma}\Delta EI\varphi_{\phi_k\gamma}\varphi''_{v_k i}\varphi''_{w_k j} & \begin{pmatrix}\bar{E}\bar{I}_v\varphi''_{v_k i}\varphi''_{v_k j} \\ +\bar{T}_k{\varphi'}_{v_k i}{\varphi'}_{v_k j}\end{pmatrix} & q_{w_k\gamma}\Delta EI\varphi''_{w_k\gamma}\varphi''_{v_k i}\varphi_{\phi_k j} & 0 \\
q_{v_k\gamma}\Delta EI\varphi''_{v_k\gamma}\varphi_{\phi_k i}\varphi''_{w_k j} & q_{w_k\gamma}\Delta EI\varphi''_{w_k\gamma}\varphi_{\phi_k i}\varphi''_{v_k j} & \begin{pmatrix}\bar{G}\bar{J}{\varphi'}_{\phi_k i}{\varphi'}_{\phi_k j} \\ +\bar{k}_a^2\bar{T}_k{\varphi'}_{\phi_k i}{\varphi'}_{\phi_k j}\end{pmatrix} & 0 \\
0 & 0 & 0 & 0
\end{bmatrix}
$$

where double subscript integer index γ implies summation from $\gamma = 1, 2, \ldots, n$. Note that all the off-diagonal submatrices are nonlinear terms. The subscript integers i and j mean the ith row and jth column of the corresponding submatrices.

Similar to the case for the kinetic energy variation, the single term in the strain energy variation,

$$
\int_0^1 \bar{T}_k\varphi'_{u_k i}\xi_k\delta q_{u_k i}d\xi \tag{D23}
$$

is used to solve for the quantity $\bar{T}_k$. Assume that the blade elongation is negligible, i.e., $\ddot{q}_{u_k i} = \dot{q}_{u_k i} = q_{u_k i} = 0$. The last rows of $\hat{M}_{k_{BR}} = \hat{M}_{k_{RB}}^T$ in Eq. (D6), $\hat{C}_{k_{BR}} = -\hat{C}_{k_{RB}}^T$ in Eq. (D10), and $\hat{K}_{k_{BB}}$ in Eq. (D13), and the quantities shown in Eqs. (D16) and (D23) produce the following equation

$$
\int_0^1 \left[\varphi_{u_k i}\left(\ddot{R}_x\mathrm{c}\theta_k - \ddot{R}_y\mathrm{s}\theta_k - \dot{R}_x\mathrm{s}\theta_k - \dot{R}_y\mathrm{c}\theta_k - 2\xi_k\dot{\vartheta}_z - 2\varphi_{v_k j}\dot{q}_{v_k j} - \xi_k\right) + \bar{T}_k{\varphi'}_{u_k i}\right]d\xi_k\delta q_{u_k i} = 0
$$

Setting the terms in the bracket to zero yields

$$\bar{T}'_k = \left(\ddot{R}_x \mathrm{c}\theta_k - \ddot{R}_y \mathrm{s}\theta_k - \dot{R}_x \mathrm{s}\theta_k - \dot{R}_y \mathrm{c}\theta_k - 2\xi_k \dot{\vartheta}_z - 2\varphi_{v_k j}\dot{q}_{v_k j} - \xi_k\right)$$

after the following integration by parts is used

$$\begin{aligned}
&\textstyle\int_0^1 \bar{T}_k \varphi'_{u_k i}\delta q_{u_k i} d\xi_k = \bar{T}_k \varphi_{u_k i}\delta q_{u_k i}\Big|_0^1 - \int_0^1 \bar{T}'\varphi_{u_k i}\delta q_{u_k i} d\xi \\
&\Rightarrow \textstyle\int_0^1 T_k \varphi'_{u_k i}\delta q_{u_k i} d\xi = -\int_0^1 \bar{T}'_k \varphi_{u_k i}\delta q_{u_k i} d\xi_k
\end{aligned}$$

with the boundary conditions, $\bar{T}_k = 0$ at $\xi = 1$ and $\delta q_{u_k i} = 0$ at $\xi = 0$. The centrifugal force can then be solved by

$$\begin{aligned}
\bar{T}_k &= -\textstyle\int_{\xi_k}^1 \left(\ddot{R}_x \mathrm{c}\theta_k - \ddot{R}_y \mathrm{s}\theta_k - \dot{R}_x \mathrm{s}\theta_k - \dot{R}_y \mathrm{c}\theta_k - 2\xi_k \dot{\vartheta}_z - 2\varphi_{v_k j}\dot{q}_{v_k j} - \xi_k\right) d\xi_k \\
&= -(1-\xi_k)\left[\ddot{R}_x \mathrm{c}\theta_k - \ddot{R}_y \mathrm{s}\theta_k - \dot{R}_x \mathrm{s}\theta_k - \dot{R}_y \mathrm{c}\theta_k\right] + \left(1-\xi_k^2\right)\dot{\vartheta}_z \\
&\quad +2\left(\textstyle\int_{\xi_k}^1 \varphi_{v_k j} d\xi_k\right)\dot{q}_{v_k j} + \frac{1}{2}\left(1-\xi_k^2\right)
\end{aligned} \tag{D24}$$

From Eqs. (D15), (D22) and (D24), the overall stiffness matrix becomes

$$\mathcal{K}_k = \begin{bmatrix}
\begin{array}{l}\bar{E}\bar{I}_w \varphi''_{w_k i}\varphi''_{w_k j} \\ +\frac{1}{2}\left(1-\xi_k^2\right)\varphi'_{w_k i}\varphi'_{w_k j} \\ -\bar{k}_{m1}^2 \varphi'_{w_k i}\varphi'_{w_k j}\end{array} & q_{\phi_k \gamma}\Delta EI \varphi_{\phi_k \gamma}\varphi''_{wi}\varphi k''_{vj} & q_{v_k \gamma}\Delta EI \varphi''_{v_k \gamma}\varphi''_{w_k i}\varphi_{\phi_k j} \\
q_{\phi_k \gamma}\Delta EI \varphi_{\phi_k \gamma}\varphi''_{v_k i}\varphi''_{w_k j} & \begin{array}{l}\bar{E}\bar{I}_v \varphi''_{v_k i}\varphi''_{v_k j} - \varphi_{v_k i}\varphi_{v_k j} \\ +\frac{1}{2}\left(1-\xi_k^2\right)\varphi'_{v_k i}\varphi'_{v_k j} \\ -\bar{k}_{m2}^2 \varphi'_{v_k i}\varphi'_{v_k j}\end{array} & q_{w_k \gamma}\Delta EI \varphi''_{w_k \gamma}\varphi''_{v_k i}\varphi_{\phi_k j} \\
q_{v_k \gamma}\Delta EI \varphi''_{v_k \gamma}\varphi_{\phi_k i}\varphi''_{w_k j} & q_{w_k \gamma}\Delta EI \varphi''_{w_k \gamma}\varphi_{\phi i}\varphi''_{v_k j} & \begin{array}{l}\bar{G}\bar{J}\varphi'_{\phi_k i}\varphi'_{\phi_k j} + \varphi_{\phi_k i}\varphi_{\phi_k j}\Delta\bar{k}_m^2 \\ +\frac{1}{2}\left(1-\xi_k^2\right)\bar{k}_a^2 \varphi'_{\phi_k i}\varphi'_{\phi_k j}\end{array}
\end{bmatrix} \tag{D25}$$

where double subscript integer γ implies summation from $\gamma = 1, 2, \ldots, n$. The elements in the off-diagonal submatrices are nonlinear and time varying in the sense that each term has involved with a time-dependent generalized coordinate. These nonlinear terms are one order in magnitude smaller than the other constant terms. However, the nonlinear terms are not negligible when the blade is subject to a constant force producing a static deflection.

System Matrices from Variation of Kinetic and Strain Energies

From Eqs. (D4) to (D7), the system mass matrix for the multiple blades is

$$\bar{\mathcal{M}} = \int_0^1 \tilde{M} d\xi; \quad \tilde{M} = \begin{bmatrix}
\bar{M}_h + \sum\limits_{k=1}^{n_b} \hat{M}_{k_{RR}} & \hat{M}_{1_{RB}} & \cdots & \hat{M}_{nb_{RB}} \\
\hat{M}_{1_{RB}}^T + \hat{M}_{1N_{BR}} & \hat{M}_{1_{BB}} & \cdots & 0 \\
\vdots & \vdots & \ddots & 0 \\
\hat{M}_{nb_{RB}}^T + \hat{M}_{nbN_{BR}} & 0 & \cdots & \hat{M}_{nb_{BB}}
\end{bmatrix} \tag{D26}$$

where $\bar{M}_h$ is the non-dimensional mass matrix of the hub and it is a diagonal matrix if the the center of hub is chosen to be the center of mass, and the hub axes are the principal axes of inertia, i.e., $\bar{M}_h = \mathrm{diag}[\bar{m}_h, \bar{m}_h, \bar{m}_h, \bar{I}_{xx}, \bar{I}_{yy}, \bar{I}_{zz}]$. Note that all the submatrices are smaller in size than the ones shown earlier because the columns and rows associated with the neglected elongation displacement of the blades u_k for $k = 1, 2, \ldots n_b$ are deleted. The size of the stiffness matrix $\mathcal{M}$ is $(6 + 3nn_b) \times (6 + 3nn_b)$.

The submatrices introduced by the centrifugal force from the strain energy are nonlinear, i.e,

$$\hat{M}_{kN_{BR}} = \begin{bmatrix} -\left(1-\xi_k\right) q_{w_k i} \varphi'_{w_k i} \varphi'_{w_k j} \mathrm{c}\theta_k & \left(1-\xi_k\right) q_{w_k i} \varphi'_{w_k i} \varphi'_{w_k j} \mathrm{s}\theta_k & 0\,0\,0\,0 \\ -\left(1-\xi_k\right) q_{v_k i} \varphi'_{v_k i} \varphi'_{v_k j} \mathrm{c}\theta_k & \left(1-\xi_k\right) q_{v_k i} \varphi'_{v_k i} \varphi'_{v_k j} \mathrm{s}\theta_k & 0\,0\,0\,0 \\ -\left(1-\xi_k\right) \bar{k}_a^2 q_{\phi_k i} \varphi'_{\phi_k i} \varphi'_{\phi_k j} \mathrm{c}\theta_k & \left(1-\xi_k\right) \bar{k}_a^2 q_{\phi_k i} \varphi'_{\phi_k i} \varphi'_{\phi_k j} s\theta_k & 0\,0\,0\,0 \end{bmatrix}$$

where the double subscript integer i implies summation from $i = 1, 2, \ldots, n$. These additional nonlinear and time-varying terms may be neglected without static deflections of the blades subject to external forces.

From Eqs. (D8) to (D11), the system gyroscopic matrix for the multiple blades is

$$\bar{C} = \int_0^1 \tilde{C} d\xi; \quad \tilde{C} = \begin{bmatrix} \bar{C}_h + \sum_{k=1}^{n_b} \hat{C}_{k_{RR}} & \hat{C}_{1_{RB}} & \cdots & \hat{C}_{nb_{RB}} \\ -\hat{C}_{1_{RB}}^T + \hat{C}_{1N_{BR}} & \hat{C}_{1_{BB}} + \hat{C}_{1N_{BB}} & \cdots & 0 \\ \vdots & \vdots & \ddots & 0 \\ -\hat{C}_{nb_{RB}}^T + \hat{C}_{nbN_{BR}} & 0 & \cdots & \hat{C}_{nb_{BB}} + \hat{C}_{nbN_{BB}} \end{bmatrix} \tag{D27}$$

where $\bar{C}_h$ is the non-dimensional gyroscopic matrix of the hub and it it is a zero matrix except, i.e., $\bar{C}_h(4,5) = \bar{I}_{zz} - \bar{I}_{xx} - \bar{I}_{yy}$ and $\bar{C}_h(5,4) = -\bar{C}_h(4,5)$. The off-diagonal nonlinear and time varying submatrices are defined by

$$\hat{C}_{kN_{RB}} = \begin{bmatrix} \left(1-\xi_k\right) q_{w_k i} \varphi'_{w_k i} \varphi'_{w_k j} s\theta_k & \left(1-\xi_k\right) q_{w_k i} \varphi'_{w_k i} \varphi'_{w_k j} c\theta_k & 0\,0\,0 & \left(1-\xi_k^2\right) q_{w_k i} \varphi'_{w_k i} \varphi'_{w_k j} \\ \left(1-\xi_k\right) q_{v_k i} \varphi'_{v_k i} \varphi'_{v_k j} s\theta_k & \left(1-\xi_k\right) q_{v_k i} \varphi'_{v_k i} \varphi'_{v_k j} c\theta_k & 0\,0\,0 & \left(1-\xi_k^2\right) q_{v_k i} \varphi'_{v_k i} \varphi'_{v_k j} \\ \left(1-\xi_k\right) \bar{k}_a^2 q_{\phi_k i} \varphi'_{\phi_k i} \varphi'_{\phi_k j} s\theta_k & \left(1-\xi_k\right) \bar{k}_a^2 q_{\phi_k i} \varphi'_{\phi_k i} \varphi'_{\phi_k j} c\theta_k & 0\,0\,0 & \left(1-\xi_k^2\right) \bar{k}_a^2 q_{\phi_k i} \varphi'_{\phi_k i} \varphi'_{\phi_k j} \end{bmatrix}$$

and the diagonal nonlinear submatrices are

$$\hat{C}_{kN_{BB}} = \begin{bmatrix} 0 & -2 q_{w_k i} \varphi'_{w_k i} \varphi'_{w_k j} \left(\varphi'''_{v_k j} \middle/ \beta_j^4 \right) & 0 \\ 0 & -2 q_{v_k i} \varphi'_{v_k i} \varphi'_{v_k j} \left(\varphi'''_{v_k j} \middle/ \beta_j^4 \right) & 0 \\ 0 & -2 q_{\phi_k i} \bar{k}_a^2 \varphi'_{\phi_k i} \varphi'_{\phi_k j} \left(\varphi'''_{v_k j} \middle/ \beta_j^4 \right) & 0 \end{bmatrix}$$

for $k = 1, 2, \ldots, n_b$. Note that double subscript integer i implies summation from $i = 1, 2, \ldots, n$. These nonlinear matrices destroy the anti-symmetry of the gyroscopic matrix. They represent only one-way coupling between the hub coordinates and the blade generalized coordinates.

From Eqs. (D12) and (D25), the system stiffness matrix for multiple blades is

$$\bar{\mathcal{K}} = \int_0^1 \hat{\mathcal{K}} d\xi; \quad \hat{\mathcal{K}} = \begin{bmatrix} \bar{K}_h + \sum_{k=1}^{n_b} \hat{K}_{k_{RR}} & \hat{K}_{1_{RB}} & \cdots & \hat{K}_{nb_{RB}} \\ \hat{K}_{1_{RB}}^T & \mathcal{K}_1 & \cdots & 0 \\ \vdots & \vdots & \ddots & 0 \\ \hat{K}_{nb_{RB}}^T & 0 & \cdots & \mathcal{K}_{n_b} \end{bmatrix} \tag{D28}$$

where $\bar{K}_h$ is the non-dimensional stiffness matrix of the hub and it it is diagonal for the principal axes, i.e., $\bar{K}_h = \text{diag}[0, 0, 0, \bar{I}_{zz} - \bar{I}_{yy}, \bar{I}_{zz} - \bar{I}_{xx}, 0]$.

Stiffness Matrix with Solar Radiation Pressure

$$\bar{\mathcal{K}} = \int_0^1 \tilde{K} d\xi; \ \tilde{K} = \begin{bmatrix} \sum_{k=1}^{n_b} \hat{K}_{k_{RR}} + \hat{K}_{kP_{RR}} & \hat{K}_{1_{RB}} + \hat{K}_{1P_{RS}} & \cdots & \hat{K}_{nb_{RB}} + \hat{K}_{nbP_{RS}} \\ \hat{K}_{1_{RB}}^T & \mathcal{K}_1 + \hat{K}_{1P_{SS}} & \cdots & 0 \\ \vdots & \vdots & \ddots & 0 \\ \hat{K}_{nb_{RB}}^T & 0 & \cdots & \mathcal{K}_{n_b} + \hat{K}_{nbP_{SS}} \end{bmatrix} \tag{D29}$$

where

$$\hat{K}_{kP_{RR}} = \begin{pmatrix} 0 & 0 & 0 & 0 & -\bar{p} & 0 \\ 0 & 0 & 0 & \bar{p} & 0 & 0 \\ 0 & 0 & 0 & 0 & 0 & 0 \\ 0 & 0 & 0 & 0 & 0 & 0 \\ 0 & 0 & 0 & 0 & 0 & 0 \\ 0 & 0 & 0 & \bar{p}\xi_k \text{c}\theta_k & -\bar{p}\xi_k \text{s}\theta_k & 0 \end{pmatrix}$$

and

$$\hat{K}_{kP_{RB}} = \begin{pmatrix} \bar{p}{\varphi'}_{w_k j} c\theta & 0 & \bar{p}\varphi_{\phi_k j} s\theta \\ -\bar{p}{\varphi'}_{w_k j} s\theta & 0 & \bar{p}\varphi_{\phi_k j} c\theta \\ 0 & 0 & 0 \\ 0 & -\bar{p}\varphi_{v_k j} c\theta & 0 \\ 0 & \bar{p}\varphi_{v_k j} s\theta & 0 \\ 0 & 0 & \bar{p}\xi_k \varphi_{\phi_k j} \end{pmatrix}$$

and

$$\hat{K}_{kP_{BB}} = \begin{pmatrix} 0 & 0 & 0 \\ 0 & 0 & \bar{p}\varphi_{v_k i}\varphi_{\phi_k j} \\ 0 & 0 & 0 \end{pmatrix}$$